ENDO-EXOCYTIC TRAFFICKING IN REGULATION OF CDC42 POLARITY

Leah Joy Watson

A dissertation submitted to the faculty at the University of North Carolina at Chapel Hill in partial fulfillment of the requirements for the degree of Doctor of Philosophy in the Department of Cell Biology and Physiology in the School of Medicine.

Chapel Hill
2014

Approved by:

Patrick Brennwald

James Bear

Keith Burridge

Adrienne Cox

Henrik Dohlman

ABSTRACT

Leah Joy Watson: Endo-exocytic Trafficking in Regulation of Cdc42 Polarity
(Under the direction of Patrick Brennwald)

The precise subcellular localization of the Rho GTPase Cdc42 is essential for its spatial and temporal control of polarized growth and division. In budding yeast, the activation and clustering of Cdc42 on the cell surface designates the site of emergence for the daughter bud and it is towards this site that the actin cytoskeleton and exocytic pathways orient to promote bud formation. In turn, exocytic delivery of Cdc42 along actin cables has been suggested as a mechanism to reinforce Cdc42's own polarized localization at the bud tip. Recycling via endocytosis and GDI-dependent mechanisms are posited to contribute to Cdc42's polarized localization by offsetting lateral membrane diffusion of Cdc42 molecules from the concentrated pool. The intimate relationship between Cdc42's function in cell polarity and the maintenance of its own localization by the pathways it regulates has been extensively studied, however, the molecular mechanisms involved in the determination and maintenance of Cdc42 polarity remain unclear.

Using a novel *in vivo* assay developed in the lab, we found that disrupting distinct stages of endocytosis severely disrupted the ability of Cdc42 to associate with secretory vesicles. This implicates the possible involvement of multiple endocytic compartments in the sorting of Cdc42 as well as the enrichment of Cdc42

into sites of endocytosis. We also demonstrate that GFP-tagged Cdc42 is highly defective in its ability to associate with vesicles. Although GFP-Cdc42 has been a valuable tool for understanding mechanisms involved in Cdc42 polarity, our findings demonstrate differences in the itineraries of the tagged and untagged Cdc42 proteins—which were previously assumed to be similar. We also demonstrate that the concentration of Cdc42 on vesicles is significantly lower than the concentrated pool on the cell surface, which demonstrates that vesicle delivery of Cdc42 is not, alone, sufficient to support Cdc42 polarity. This provides the first direct experimental support for a negative regulatory role for vesicle transport in Cdc42 polarity.

To my supportive parents, my grandmother and departed loved ones

"*…you'll always be my Joy*"

ACKNOWLEDGEMENTS

First, I must thank God. Throughout graduate school, I have had to face many deaths in my family, a failed thesis project, many personal losses and frustrations. However, my faith has been essential for me to overcome every challenge, appreciate every lesson and delight in my successes no matter the scale.

Thank you to my advisor, Dr. Patrick Brennwald. You taught me to extract lessons from every failure and success, to exploit imperfections in the attempt for perfection, and to question everything. I am forever grateful for your lessons, both intentional and unintentional.

Thank you to my committee members: Drs. Jim Bear, Keith Burridge, Adrienne Cox and Henrik Dohlman. Your advice and guidance during each of our meetings have been important to my development as a scientist.

The last seven years in the Brennwald lab would not have been as enjoyable without my fellow lab mates, especially Drs. Guendalina Rossi and Hao Wu. Thank you, Rossi for your experimental and intellectual contributions to my research, your encouragement, support and laughter. Most of all, thank you for your friendship. Your cheerfulness and good-humor have been sunshine to many gloomy days. Thank you, Hao for your guidance and support during my first few years in the lab. I will always cherish and appreciate your friendship. Thank you to my bench mate and

“little sister”, Kelly Watson, for critical readings of my manuscript, for giving me someone to laugh at (with), and for your support.

To my coffee buddies: Drs. Michelle Itano, Meghan Morgan-Smith and Katie Wolfe. For your friendship, for your laughter, for being there…Thank you.

Thank you to all of my UNC network, friends, and family for their support and encouragement throughout my time at UNC, especially: Kyle McKenna, Ashalla Freeman, Pat Phelps, Michael Johnson, Sabrice Guerrier, the IMSD/STAD/TIBBs/BBSP office, Alan Anderson, Marva Taylor, Monique Sprueill, and MoniQue Honablew.

To my loving parents and grandmother: your unconditional love, support, belief in me, and encouragement will forever be my safe place.

TABLE OF CONTENTS

LIST OF FIGURES AND TABLES

LIST OF ABBREVIATIONS

RHO	Ras HOmolog
CDC42	Cell Division Cycle 42
RSR1	RaS-Related 1
GEF	Guanine nucleotide Exchange Factor
GAP	GTPase-Activating Protein
GDI	GDP Dissociation Inhibitor
CDC24	Cell Division Cycle 24
RGA1/2	Rho GTPase Activating Protein
BEM1/2/3	Bud EMergence
RDI1	Rho GDP Dissociation Inhibitor
FRAP	Fluorescence Recovery After Photobleaching
LatA/B	LATrunculin
TGN	Trans Golgi Network
ROI	Region Of Interest
GFP	Green Fluorescent Protein

CHAPTER 1: Introduction and Background

1.1 Overview

Cell polarity is defined as the partitioning of cellular materials into spatially distinct domains in response to external and/or internal stimuli. Virtually all cells polarize at some point during their lifetime. Whether to grow and divide or to perform highly specialized cellular functions such as axonal migration or activation of the immune response, the process of cell polarization is a critical component of eukaryotic cell biology [1-4].

Much of the current understanding of polarity and the identification of many key regulators can be attributed to studies using the budding yeast *Saccharomyces cerevisiae*. Polarity in budding yeast essentially is compartmentalizing the cell into a distinct cell “front” and “back” during either the production of a daughter bud or a mating projection. In particular for budding, the proper establishment of a cell “front” ensures that only one bud is constructed per cell cycle [2, 5]. Besides the pronounced polarization state during most of their life cycle, budding yeast are a genetically tractable system with many conserved key components of polarity. As such, budding yeast are an excellent model system for dissecting the mechanisms underlying cell polarity.

Among the conserved regulators of polarity, the Rho family of the Ras superfamily of GTPases are crucial determinants of the establishment and maintenance of the polarized axis in yeast [6-10]. Rho GTPases have an

evolutionarily conserved role in defining the cell “front” and “back”. They are important for several physiological processes—including axonal migration, membrane trafficking, actin organization, and morphogenesis—and pathological processes that include metastasis, cell survival and infinite proliferative potential [11, 12]. The Rho GTPase, Cdc42, is essential for polarity establishment in yeast [9, 10, 12, 13]. Its local activation at the plasma membrane designates the cell “front” or the site where the daughter bud will form [14, 15]. This chapter will discuss the establishment of polarity in yeast, the identification and characterization of Cdc42 as the “master regulator of polarity”, the link between the localization of Cdc42 and bud emergence, and gaps in the current knowledge of Cdc42 polarity wherein my work will endeavor to fill.

1.2 Establishment of cell polarity in budding yeast

Polarity establishment generally involves 1) a cellular response to intrinsic/extrinsic stimuli, 2) determination of a single, defined polarity axis direction and 3) construction of the axis via positioning of polarity factors and pathways towards a spatial landmark [12]. The commitment to exit isotropic growth and trigger asymmetry in yeast results in either the formation of a bud or shmoo/mating projection [2, 16]. The polarization “trigger” and polarity axis determinant are different for each of these forms of asymmetry. For example, the trigger and direction of polarization during mating are both determined by a pheromone gradient, whereas, budding is initiated by the cell-cycle program (START) and the polarity axis is spatially defined by the general bud site selection machinery [2].

Budding yeast display two spatial patterns for placement of the nascent bud and subsequent separation from the mother. The bud of haploid yeast cells forms adjacent to the previous division site (axial budding pattern), while the bud forms at the polar opposite end of the previous division site (bipolar budding pattern) in diploid cells. Axial and bipolar budding patterns are dictated by distinct "landmark" proteins which are passed along from mother to nascent bud. Axial budding requires the gene products of *BUD3*, *BUD4*, *AXL1*, and *AXL2/BUD10*, whereas the gene products of *BUD7*, *BUD8*, *BUD9*, *RAX1*, and *RAX2* are specific for the bipolar budding pattern [13, 15, 17-19]. The gene products of *RSR1/BUD1*, *BUD2*, and *BUD5* comprise a general bud selection machinery that is involved in both axial and bipolar budding [13, 15, 17, 20]. After the initiation of the cell-cycle program, the procession of polarity establishment follows: 1) the general selection machinery (*RSR1/BUD2/BUD5*) interprets the axial and bipolar signal for bud placement 2) transmits these spatial coordinates to the polarity establishment machinery then 3) the polarity establishment machinery organizes the actin cytoskeleton and delivery of protein and vesicles towards this site on the cell surface to promote bud emergence.

Although the polarity establishment machinery responds to the spatiotemporal cues transmitted by the bud site selection machinery to spatially restrict polarity to the defined bud site, the bud site selection genes are nonessential. In fact, studies utilizing mutants that remove spatial landmarks (i.e. *BUD3-4/BUD7-9/AXL1-2/RAX1-2* gene deletions) or the transmission of the landmark signal (i.e. *rsr1*Δ) demonstrate that polarity can effectively be established along any axis [17, 21]. This suggests that

cells are inherently capable of switching from symmetrical to asymmetrical growth—albeit in a randomized orientation. Further examination of the establishment of polarity in yeast led to the characterization of the polarity establishment machinery which is comprised of the Cdc42 GTPase and its regulators (i.e. Cdc24, Rga1, Rga2, Bem2, and Bem3). The consensus of these studies has led to the classification of Cdc42 as the central or "master" regulator of polarity [22], and as such, massive efforts remain focused on dissecting its function in polarized growth.

1.3 Identification and characterization of Cdc42 as the "master regulator of polarity"

The Rho GTPase *CDC42* was originally identified from an extensive screen for mutants with growth arrest phenotypes resembling previously characterized mutations in the gene *CDC24* [9, 10, 23, 24]. The *cdc42-1* temperature sensitive mutant isolated from this screen displayed defects in actin cable distribution despite normal isotropic growth at the restrictive temperature of 37^{o}C. This mutant also failed to form buds at the restrictive temperature—resulting in cells with a large, round morphology similar to the *CDC24* mutants [9, 23, 24]. Interestingly, *CDC42* and *CDC24* single null mutants are both inviable in *S. cerevisiae* and *S. pombe* [10, 25]. *CDC42* was later identified in mammals [26] and knockout mice were embryonic lethal [27]. Given the previously reported involvement of Cdc24 in polarized growth and the similarities between *CDC42* and *CDC24* mutants, these observations provided the first indication of their essential roles in polarized growth and bud emergence.

The Cdc42 GTPase, like other GTPases, cycles between active, guanine triphosphate (GTP)-bound and inactive, guanine diphosphate (GDP)-bound states. GTPases are activated by guanine nucleotide exchange factors (GEFs) which stimulate the release of GDP and loading of GTP. Follow-up studies to the aforementioned screen revealed Cdc24 as the sole GEF for yeast Cdc42 [12, 28]. The GTPase activating proteins (GAPs)—Bem2, Bem3, Rga1 and Rga2—inactivate Cdc42 by catalyzing its intrinsic ability to hydrolyze GTP [28]. Studies using nucleotide-locked forms of Cdc42 reveal the requirement for its GTPase cycle in cell viability, the establishment of a single "front" or bud per cell cycle, and its ability to localize properly [29-32].

Rho guanine nucleotide dissociation inhibitors (GDIs) offer yet another layer of regulation for Rho GTPases. Rho GDI proteins, so named due to their ability to inhibit the dissociation of GDP from the GTPase, also inhibit Rho proteins' intrinsic and GAP-stimulated GTP hydrolysis [15]. A third function of Rho GDIs is to extract Rho proteins from membranes into the cytosol [15]. GDI-mediated extraction solubilizes Rho proteins by concealing an N-terminal lipid moiety (*see Cdc42 localization and polarity*) of the GTPase within the hydrophobic pocket of the GDI protein. The sole yeast Rho GDI Rdi1 inhibits nucleotide dissociation and extracts GDP-bound Rho proteins from membrane compartments [15, 33]. Despite the function of Rdi1 in regulating Rho protein attachment to membranes, *RDI1* is nonessential. The seemingly lack of a phenotype in an *rdi1*Δ strain implies it is not essential for Cdc42 or other Rho protein function. This is surprising considering membrane attachment is a critical aspect of Rho GTPase function. However,

studies reveal that Rdi1-mediated rapid recycling of Cdc42 from the plasma membrane is involved in maintaining the plasma membrane localization of Cdc42. Furthermore, the lethality imparted by *RDI1* overexpression [34] strongly suggests Rdi1 could negatively impact Cdc42 function via unrestricted extraction of the GTPase from membranes [35, 36].

In the hierarchal order of polarity, the regulation of Cdc42 activity and membrane attachment by its GEF, GAPs and GDI are integral components of polarity establishment following selection of the site of bud emergence. The bud site selection machinery transmits the spatial coordinates of the designated bud site directly to the Cdc42 GTPase and its GEF Cdc24. This ultimately results in the recruitment and clustering of activated Cdc42 to this site on the cell surface. The subsequent orientation of the actin cytoskeleton and vesicle trafficking pathways towards this site begins the construction of the daughter bud (Figure 1.1). Membrane trafficking and Rdi1-mediated recycling of Cdc42 to this site are considered parallel mechanisms for maintaining Cdc42 at the bud site to continue membrane expansion during bud formation (see *Cdc42 localization and polarity*). Although the defined bud site—as selected by the landmark proteins—biases the location of Cdc42 clustering, the removal of spatial cues merely randomizes the site of bud placement rather than prevents bud emergence altogether [14, 15]. This ability of yeast cells to break symmetry *de novo* was found to be entirely dependent on the localization of Cdc42. Thus, the polarized localization of Cdc42, not upstream factors, is necessary and sufficient for determining the site of bud emergence.

1.4 Cdc42 localization and polarity

Wu *et al*. [37] demonstrated that the distinct localizations of Cdc42 and another Rho protein, Rho3, are integrated into their function such that their localizations reflect the stages at which each GTPase regulates polarized growth. As the determinant of bud emergence and formation, Cdc42 localizes as a concentrated cap on the plasma membrane at the presumptive bud site of unbudded cells and the bud tip of small budded cells. Cdc42 disperses around the cell periphery as the bud enlarges, only to re-cluster at the mother-bud neck prior to its regulation of cytokinesis (Figure 1.2) [12, 37]. Prenylation of the carboxyl-terminal CAAX moiety (A is aliphatic amino acid; X is any amino acid) of Cdc42 is required for its peripheral attachment to membranes. The ^{188}Cys residue in the CAAX domain is prenylated via the addition of a C_{20} geranylgeranyl isoprene group and mutational analysis of this domain revealed the requirement of prenylation for Cdc42 activity and function [31].

The Rho3 GTPase, on the other hand, is prenylated by the addition of a C_{15} farnesyl isoprene group to its CAAX motif, but the palmitoylation of an N-terminal cysteine is important for determining its distinct localization pattern [37]. Rho3 localizes to the mother cell periphery in unbudded and small budded cells. Its localization is constrained to the bud periphery during bud enlargement—reflecting its regulatory role in the later stages of bud growth (Figure 1.2) [37]. As the distinct localizations of Rho proteins likely affects their capacity to engage different effector pathways in a spatiotemporal manner, understanding the mechanism(s) by which Rho proteins localize and maintain localization is key to understanding their control of polarized growth.

The isotropic-asymmetric switch in Cdc42 plasma membrane localization is thought to involve two distinct positive feedback loops: the adaptor-based signaling and the actomyosin-based transport systems. Both systems are thought to generate and maintain robust Cdc42 polarity by amplifying a spontaneously occurring cluster of GTP-Cdc42 on the cell surface [38-41]. For example, active Cdc42 binds to a signaling complex consisting of the adaptor, scaffold protein Bem1 (Bud EMergence 1), the GEF Cdc24 and a p21-activated kinase (PAK)-family kinase. As a result of its interaction with the GEF-Bem1-PAK complex, neighboring GDP-bound Cdc42 molecules become activated and thus ensues the perpetual recruitment of GEF-Bem1-PAK complexes and local activation of Cdc42 at the presumptive bud site.

In the case of actomyosin-based transport, a stochastically-generated cluster of active Cdc42 orients actin cable nucleation via localized formin activation [42, 43]. Actin cables serve as tracks for myosin-mediated transport of Cdc42-laden post-Golgi vesicles. The delivery and fusion of secretory vesicles carrying Cdc42 with the active pool at the plasma membrane reinforces further local activation of GDP-Cdc42 on the cell surface and drives membrane expansion.

Previous studies using fluorescence recovery after photobleaching (FRAP) revealed the rapid cycling of GFP-Cdc42 between the plasma membrane and internal membrane compartments [30, 44]. These data indicate that the pool of activated Cdc42—or the Cdc42 polarity cap—is dynamically maintained [30, 44, 45]. Indeed, lateral diffusion of Cdc42 within the lipid bilayer can easily dilute the concentration of the polarity cap if the positive feedback systems described above are not counteracted. Two mechanisms to circumvent lateral diffusion via continuous

cap-cytosol exchange have been proposed. First, endocytic recycling of Cdc42 from the plasma membrane polarity cap counterbalances its delivery on post-Golgi secretory vesicles. Irazoqui *et al*. found that the partial depolymerization of F-actin structures using Latrunculin B (Lat B) results in the dispersal of Cdc42 from the plasma membrane polarity cap [45]. Furthermore, disruption of endocytosis, not *RDI1*, prevented Lat B-induced Cdc42 dispersal. Co-fractionation studies reveal the association of Cdc42 with both classes of secretory vesicles, Bgl2 and invertase, of which invertase-containing vesicles are known to initially sort through endosomes before entering another round of exocytosis [46]. Second, Rdi1 binds to and extracts prenylated GDP-Cdc42 from membrane compartments into the cytosol. Deletion of *RDI1* significantly depletes the cell of cytosolic Cdc42 [47], whereas, overexpression of *RDI1* dramatically increases the levels of cytosolic Cdc42 resulting in cell lethality [48].

1.5 Gaps in current understanding

Notwithstanding the breadth of research dedicated to elucidating mechanisms involved in Cdc42 polarization, gaps in our current understanding still remain. In the actin-based transport model, it is the delivery and fusion of secretory vesicles carrying Cdc42 with the plasma membrane polarity cap that is thought to maintain Cdc42's polarized localization [49]. However, a major criticism of this model is that Cdc42 must diffuse relatively slowly within the plasma membrane bilayer and be concentrated on vesicles in amounts that either compare to or exceed the polarity cap in order for membrane trafficking to sustain polarity (Figure 1.3) [50]. Given the fraction of native, untagged Cdc42 associated with vesicles compared to the polarity

cap is unknown, assessing the contribution of membrane trafficking has been challenging. Although recycling of Cdc42 by Rdi1 and endocytosis are presumably partially redundant pathways, neither endocytic uptake of GDP-Cdc42 nor the accessibility of the vesicular pool of Cdc42 for Rdi1 extraction have been demonstrated. Furthermore, the difference between bulk and selective incorporation of Cdc42 into the endocytic pathway is still unclear. In light of these and other key concerns, the direct assessment of the contribution of membrane trafficking pathway to Cdc42 polarity will aid in further understanding Cdc42's control of polarized growth.

1.6 Figures

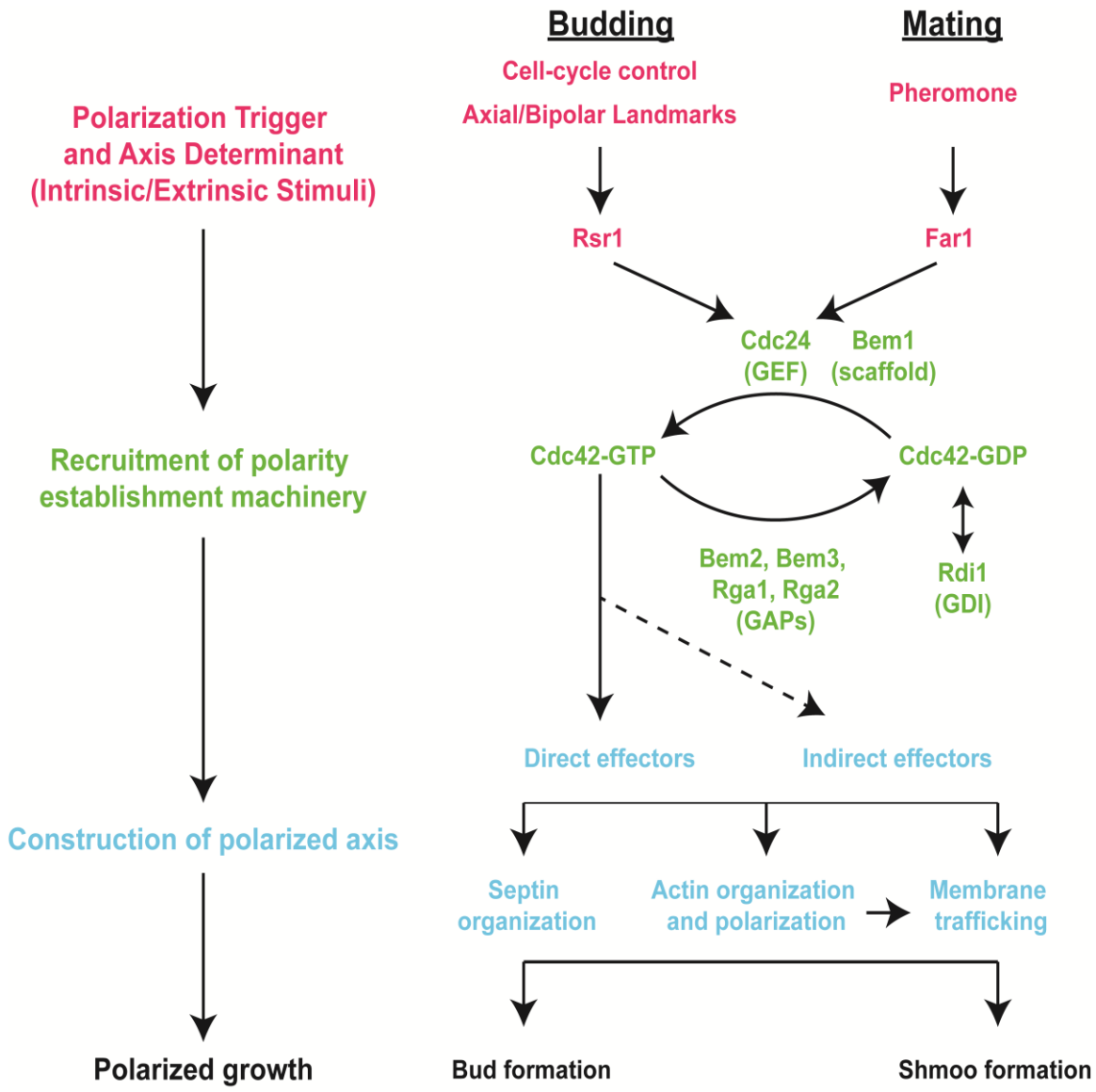

Figure 1.1 Hierarchal model for polarity establishment in budding and mating cells. Polarization trigger and axis determinant (fuchsia): spatial landmark proteins or pheromone signals are interpreted and conveyed to the Cdc42 GTPase module (green). Recruitment of polarity establishment machinery: the Cdc42 GEF, Cdc24 activates Cdc42 leading to the generation and maintenance of a pool of GTP-Cdc42 on the cell surface (green). Construction of polarized axis: active Cdc42 engages downstream direct and indirect effectors to coordinate the organization of septins (blue), actin cytoskeleton (red) and membrane trafficking (yellow) during bud or shmoo (mating projection) formation.

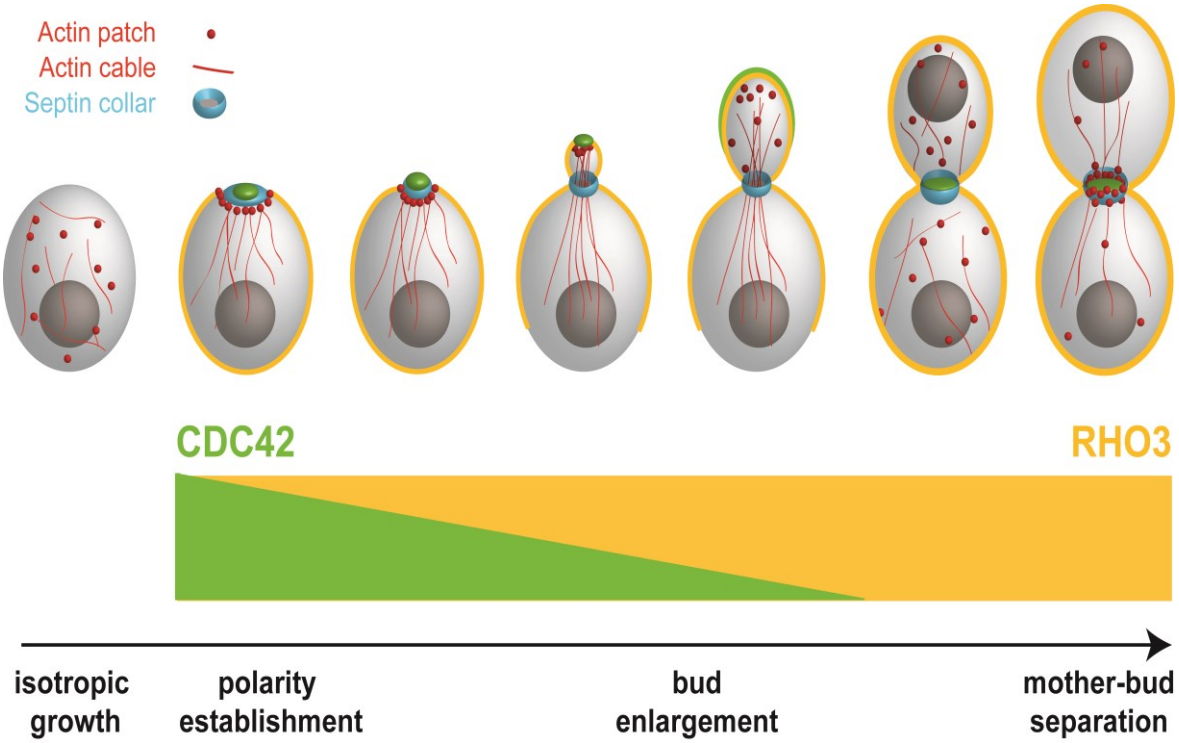

Figure 1.2 Rho GTPase localization and polarized growth. The re-localization of Cdc42 and Rho3 throughout the cell cycle reflects the stages at which they control polarized growth. The organization of the actin cytoskeleton and membrane expansion (via polarized exocytic transport) are targeted by Cdc42 towards the bud tip during bud formation and growth and redirected towards the mother-bud neck prior to cell separation (Cdc42's function in septin and actin organization). Rho3 localizes around the mother cell periphery in unbudded cells and, to some extent, becomes restricted to the bud periphery as the bud enlarges (reflecting Rho3's function in the later stages of bud growth). Adapted from [14, 15, 51, 52].

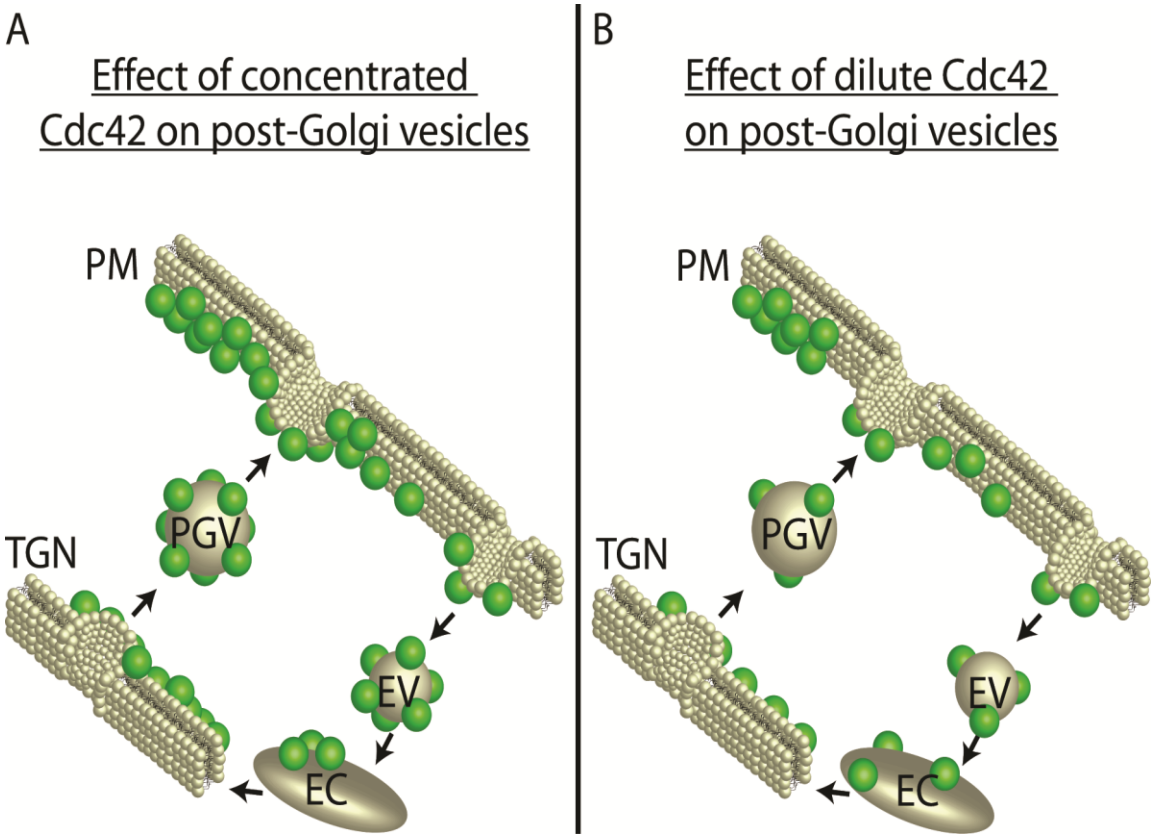

Figure 1.3 Schematic representation of potential outcomes of the delivery of post-Golgi secretory vesicles (A) sufficiently and (B) insufficiently loaded with Cdc42. Abbreviations: plasma membrane (PM); Trans Golgi Network (TGN); post-Golgi secretory vesicle (PGV); endocytic vesicle (EV); endosomal compartment (EC). Membrane compartments (gray); Cdc42 molecules (green).

CHAPTER 2: Quantitative Analysis of Membrane Trafficking in Regulation of Cdc42 Polarity[1]

2.1 Overview

Vesicle delivery of Cdc42 has been proposed as an important mechanism for generating and maintaining Cdc42 polarity at the plasma membrane. This mechanism requires the density of Cdc42 on secretory vesicles to be equal to or higher than the plasma membrane polarity cap. Using a novel method to estimate Cdc42 levels on post-Golgi secretory vesicles in intact yeast cells, we: 1) determined that endocytosis plays an important role in Cdc42's association with secretory vesicles 2) found that a GFP-tag placed on the N-terminus of Cdc42 negatively impacts this vesicle association and 3) quantified the surface densities of Cdc42 on post-Golgi vesicles which revealed that the vesicle density of Cdc42 is three times more dilute than that at the polarity cap. This work suggests that the immediate consequence of secretory vesicle fusion with the plasma membrane polarity cap is to dilute the local Cdc42 surface density. This provides strong support for the model in which vesicle trafficking acts to negatively regulate Cdc42 polarity on the cell surface while also providing a means to recycle Cdc42 between the cell surface and internal membrane locations.

[1] Reproduced with permission from: Watson, L.J., Rossi, G., and Brennwald, P. (2014). Quantitative Analysis of Membrane Trafficking in Regulation of Cdc42 Polarity. Traffic. DOI: 10.1111/tra.12211

2.2 Introduction

Growth along a defined axis is important for many biological processes. The subcellular localizations of key regulators and effectors of polarity are intricately linked with their control of the establishment and maintenance of the polarized axis [14, 37, 49, 53]. In budding yeast, the switch from isotropic to asymmetric growth is preceded by the accumulation of activated (GTP)-Cdc42—a conserved Rho GTPase—at the presumptive bud site [12, 15]. The Cdc42 polarity cap is required to orient the actin and secretory pathways toward the nascent bud site and Cdc42 polarization is necessary and sufficient for determining the site of bud emergence [14, 49].

Generation and maintenance of robust Cdc42 polarity promotes membrane expansion during bud formation. Studies reveal that Cdc42 is dynamically maintained at the polarity cap through its continuous cycling between the polarity cap and internal pools [30, 44, 45]. Two major mechanisms for recycling Cdc42 have been described. In one mechanism, GDP-Cdc42 is rapidly recycled by the sole yeast Rho GDP dissociation inhibitor, Rdi1. In the other proposed mechanism, actomyosin-based exocytic delivery of Cdc42 is coupled to a slower endocytic retrieval pathway. Both mechanisms presumably circumvent the lateral membrane diffusion of Cdc42 by coupling Cdc42 delivery to a localized GEF-mediated positive feedback system [45, 46, 54-56]. Although endogenous Cdc42 has been shown to associate with secretory vesicles [46, 57, 58], a recent report using mathematical modeling challenges a possible role for membrane trafficking in polarizing Cdc42 [50]. Common methods for estimating the vesicle-bound pool of Cdc42 either

subject cells to lysis conditions or require fluorescently tagged protein—both of which may impede direct quantitative assessment of the membrane association of the native protein.

In this study, we make use of a novel assay to quantitatively assess the contribution of the recycling pathways to the polarity of endogenous Cdc42 and obtain estimations of the relative and absolute concentrations of Cdc42 on post-Golgi vesicles and the plasma membrane polarity cap. While our results implicate endocytic and exocytic trafficking in recycling of Cdc42, they also demonstrate that the density of Cdc42 protein on exocytic vesicles is significantly lower than at the plasma membrane polarity cap. We discuss the implications of these findings on current models for Cdc42 polarization.

2.3 Results

2.3.1 A quantitative assay for Cdc42-vesicle association

Previous work utilizing thin section electron microscopy demonstrated that *GAL*-induced overexpression of either of two Sec4 effector proteins, Sec15 or Sro7, results in the formation of a large, homogeneous cluster of tightly, compacted 80-100 nm post-Golgi secretory vesicles within the cytosol [59-61]. We made use of this observation to establish a novel *in vivo* assay for quantitatively examining the association of Cdc42 with post-Golgi vesicles as a complement to earlier studies that used subcellular fractionation and other biochemical methods for vesicle purification [46, 57, 58]. As observed previously, *GAL*-induced overexpression of either Sec15 or Sro7 results in a marked change in the localization of Sec4 from sites of polarized growth to a large cytoplasmic patch within the cell which corresponds to a cluster of

post-Golgi vesicles observed by thin section electron microscopy [59-61] (Figure 2.1A). Consistent with results from biochemical studies, double-labeled immunofluorescence staining with antibodies directed at Cdc42 and Sec4 revealed a striking re-localization of Cdc42 from the bud-tip to the Sec4-positive vesicle clusters in response to the Sec15 or Sro7 induction (Figure 2.1A). In both Sec15- and Sro7-induced cells we find that all the cytoplasmic clusters that are positive for Cdc42 are also positive for Sec4 and that greater than 70% of Sec4-positive clusters were positive for Cdc42 (Figure 2.1B). This is the similar to the level of co-localization observed at the plasma membrane polarity cap in uninduced cells (*GAL*-vector, Figure 2.1B).

As a first step in the quantification of Cdc42 levels found on specific membrane compartments, we measured the ratio of Cdc42 fluorescence associated with Sec4-positive vesicle clusters or the plasma membrane polarity cap to an equivalent-sized region in the cytoplasm. The relative Cdc42 fluorescence associated with vesicle clusters was greater than (*GAL-SEC15*) or similar to (*GAL-SRO7*) that seen for the polarity cap observed in control (*GAL*-vector) cells (Figure 2.1C). Therefore, Cdc42 appears to be present on post-Golgi vesicles at levels comparable to the plasma membrane polarity cap. However to properly address the question posed by the trafficking model concerning the relative concentration of Cdc42 on vesicles compared to the plasma membrane polarity cap, it was important to also take into careful consideration the membrane surface areas contributing to each of these fluorescence measurements (see section on quantification of Cdc42 densities below).

2.3.2 Endocytosis is required for Cdc42 post-Golgi vesicle association

Recycling of Cdc42 to and from the plasma membrane polarity cap is thought to be critical to its ability to act in cell polarization. Two mechanisms for Cdc42 recycling have been proposed. One mechanism involves the Rho GDI protein which selectively extracts the GDP-bound form of geranylgeranylated Cdc42 from the plasma membrane by providing a pocket for the hydrophobic prenyl group—similar to the role for Rab GDI in Rab GTPase recycling [62]. The second mechanism involves endocytic recycling of Cdc42 from the plasma membrane in a pathway that may function in parallel to its recycling by Rho GDI [44, 45, 63]. We made use of the vesicle clustering assay described above to examine the requirement of GDI or endocytosis in the association of Cdc42 with post-Golgi vesicles. To examine the endocytic requirement, we disrupted endocytosis using a deletion in *END4* (also known as *SLA2*) which regulates the interaction between endocytic vesicles and the actin cytoskeleton during vesicle internalization [64]. As expected (Figure 2.2A), Cdc42 localization at the plasma membrane polarity cap is stable in cells lacking *RDI1* or *END4* [44-47]. However, induction of vesicle clusters in an *end4*Δ background resulted in >60% reduction in the relative concentration of Cdc42 associated with vesicle clusters in Sro7- or Sec15-overexpressing cells (Figure 2.2B, C, E and F). Examination of the penetrance of this phenotype demonstrated that greater than 70% of cells exhibited a dramatic reduction (by more than 50%) in the levels of Cdc42 present in the Sec4-positive vesicle clusters (Figure 2.2D, G). Disruption of *RDI1* function did not negatively affect cluster association of Cdc42 in either Sro7- or Sec15-overexpressing cells (Figure 2.2B through G). Indeed, *rdi1*Δ

cells had increased levels of Cdc42 associated with vesicles—which is consistent with the documented depletion of cytosolic Cdc42 in *rdi1*Δ cells [44, 46, 47]. Therefore, while endocytosis is important for Cdc42 association with post-Golgi vesicles, Rho GDI is completely dispensable for this association.

We next examined the association of Cdc42 with vesicle clusters in mutants known to have defects at distinct points in endocytic trafficking from the plasma membrane to endosomes and the Trans Golgi Network (TGN). Sla1, like End4, functions at the plasma membrane during endocytic vesicle formation, while Tlg2 and Pep12 are important for transport between the early endosome to the TGN and between the late endosome (or PreVacuolar Compartment) and the TGN, respectively [65]. We found that defects in any of these gene products results in a significant and highly penetrant defect in Cdc42 association with vesicle clusters, suggesting that Cdc42 recycling onto post-Golgi vesicles is likely to involve trafficking through multiple endocytic compartments (Figure 2.3A, B).

Cdc42 has previously been shown to associate with post-Golgi vesicles that accumulate in response to a *sec6-4* mutation when analyzed by differential centrifugation [57]. To examine the role of endocytic and GDI-mediated recycling on the association of Cdc42 with post-Golgi vesicles by differential centrifugation, we constructed double mutants of *rdi1*Δ or several endocytic mutants with *sec6-4.* In response to a *sec6-4* mutation, cells shifted to 37^{o}C accumulate post-Golgi secretory vesicles which pellet selectively at 100,000 x g (P100). This effect is observed by a large increase in the levels of Sec4 in the P100 fraction in a *sec6-4* strain compared to control wild-type cells. Consistent with previous reports [46, 57], an increase in

Cdc42 association with the P100 fraction also occurs in response to the secretory vesicle accumulation (Figure 2.3C, D). We also observed that when *rdi1*Δ, *sec6-4* cells were examined, elevated levels of Cdc42 were maintained in the P100 fraction. In contrast, the P100 fraction of *pep12*Δ, *sec6-4* mutants—despite having normal accumulation of Sec4—was depleted of Cdc42 compared to *sec6-4* cells (Figure 2.3C, D). The accumulation of secretory vesicles in the *end4*Δ, *sec6-4* double mutant was problematic and, unfortunately, this mutant could not be utilized for analysis by fractionation. Nonetheless, the results of fractionation clearly confirm both a role for endocytic recycling and the lack of a requirement for GDI function in the association of Cdc42 with exocytic vesicles.

2.3.3 GFP-Cdc42 shows impaired association with post-Golgi vesicles

Previous work from our lab has demonstrated an important role for the N-terminus of Rho family GTPases in determining their patterns of subcellular localization [37]. Perhaps not surprisingly, several groups have demonstrated significant growth defects associated with N-terminal GFP-tagged forms of Cdc42 expressed as the sole source of Cdc42 in the cell [55, 66, 67]. Since the work described above relied exclusively on untagged Cdc42 expressed from its endogenous chromosomal locus, we examined the effect of a GFP-tagged form of Cdc42 on its association with post-Golgi vesicles in our vesicle clustering assay. We generated strains containing *GAL-SEC15* with either GFP-tagged or untagged *CDC42* expressed behind their native promoter on a *CEN/LEU2* plasmid as the sole source of *CDC42*. Expression from the *CEN* plasmids results in a slight, but equivalent, increase in overall Cdc42 levels (Figure 2.S1D). Although both

constructs show normal growth and polarization at 25°C (Figure 2.4A, B), the GFP-tagged form of Cdc42 resulted in lethality at 37°C as previously reported (Figure 2.S1A, 2.4D) [55, 66, 67]. When induced with galactose, we saw the expected staining of untagged Cdc42 on the large cytoplasmic puncta co-stained by Sec4. However, the strain containing the GFP-tagged form of Cdc42 demonstrated very weak staining of these puncta that was only slightly above the levels of the surrounding cytoplasm (Figure 2.4A, C). These data indicate that the presence of a GFP tag on the N-terminus of Cdc42 results in a dramatic loss of post-Golgi vesicle association in this assay.

As mentioned above, Slaughter *et al*. [44] have proposed two parallel mechanisms for recycling of Cdc42: 1) Rdi1-mediated membrane extraction and re-delivery through the cytosol and 2) endocytic uptake and redelivery on exocytic vesicles. A clear prediction of this model is that loss of the sole Rho GDI in yeast should demonstrate synthetic growth defects when combined with a form of Cdc42, in this case GFP-Cdc42, which disrupts its association with exocytic vesicles. We therefore utilized a plasmid shuffle assay to examine the effect of an *rdi1*Δ on the ability of GFP-Cdc42 to function as the sole source of Cdc42 in the cell. Previous reports have demonstrated that GFP-Cdc42 is unable to support growth at high temperatures [55, 66, 67]. We find that the temperature-sensitive nature of GFP-Cdc42 is accentuated by the presence of *rdi1*Δ. In particular, the synthetic effect of the GFP tag and loss of Rho GDI is most apparent at 34.5°C, a temperature at which GFP-Cdc42 is viable with *RDI1* (Figure 2.4D). While this synthetic sickness at 34.5°C is consistent with the parallel functions for endocytosis and *RDI1*, the viability

at ambient temperatures and the sustained polarized localization also suggests that there may be a third mechanism for recycling Cdc42 that is independent of both *RDI1* and endocytic/exocytic recycling.

2.3.4 Quantification of Cdc42 density on vesicles and the plasma membrane polarity cap

While previous studies using subcellular fractionation as well as the immunofluorescence studies described above have established that Cdc42 is associated with post-Golgi vesicles in significant amounts, the precise density of Cdc42 molecules on the surface of these vesicles has not been determined. The vesicle clustering procedure described above presented a unique opportunity to address this question *in vivo*, without the numerous difficulties—such as degradation and membrane disassociation—that are often associated with biochemical fractionation. Therefore, we set out to determine the absolute density of Cdc42 molecules on both post-Golgi vesicles (within the clusters) as well as at the plasma membrane polarity cap. This required having reliable estimates of: 1) the total number of molecules of Cdc42 in the cell 2) the membrane surface area associated with the vesicle clusters or the plasma membrane polarity cap and 3) the fractional amount of Cdc42 associated with each of these two regions.

Surprisingly, we were unable to find a direct estimate of Cdc42 copies per cell in whole proteome-tagging studies [68] or other published work. We therefore generated our own estimate by a ratio-metric comparison of GFP fluorescence of a yeast strain containing GFP-Cdc42 on a *CEN* plasmid with a reference strain containing a GFP-tagged form of the kinetochore protein Cse4—of which the copy

number per sister kinetochore cluster is well established [69-71]. To compare the relative fluorescence levels of GFP-Cdc42 in the total cell and Cse4-GFP in the sister kinetochore clusters, the two strains were mixed and imaged by fluorescence microscopy (Figure 2.5A). With each sister kinetochore containing 80 copies of Cse4, the resulting comparison yielded an estimate of roughly 27,400 copies of GFP-Cdc42 per cell. We then compared the amount of plasmid-derived GFP-Cdc42 to that of endogenous Cdc42 in wild type cells by quantitative Western blot analysis (Figure 2.5B). From this analysis we estimate that wild type cells contain approximately 6,800 copies of Cdc42 per cell.

Since the growth conditions for the vesicle clustering assays differed from the above conditions, we compared the effects of carbon source and vesicle clustering on Cdc42 amounts per cell. While we found there was little effect of carbon source (glucose vs. raffinose; data not shown) on the levels of Cdc42, there was a significant (>50%) increase in Cdc42 amounts in strains when vesicle clusters were induced (Figure 2.5C). This is presumably due to the enlargement of cells and the inhibition of cell division during vesicle cluster formation. Based on this comparison, we estimate approximately 10,400 copies of Cdc42 per cell following the 8 hour galactose induction of Sec15—identical to the conditions used for fluorescence imaging.

We next utilized morphometric analysis of thin-section electron micrographs to determine the packing density of post-Golgi vesicles associated with *GAL-SEC15* and *GAL-SRO7* induced vesicle clusters used for fluorescence imaging (Figure 2.5E, F). This analysis demonstrated that the vesicle clusters contained

approximately 35.5 ± 3.9 post-Golgi vesicles (90nm average diameter) per square micron for each thin section. Thus, the 0.718 micron diameter regions of interest (ROI) used for fluorescence imaging (0.2μm thick optical sections) of clusters corresponded to approximately 71 vesicles or a total vesicle membrane surface area of 0.723 square microns per ROI. Fluorescence microscopy was used to determine the fractional amount of Cdc42 (% of total) associated with each ROI. Considering the total copy number of Cdc42 in the cell, our assessment yielded ~187 copies of Cdc42 in the vesicle cluster ROI. This corresponds to approximately 6.5 copies of Cdc42 per vesicle or a density of ~260 copies of Cdc42 per square micron of vesicle surface (Figure 2.5E, G).

To assess Cdc42 surface density at the plasma membrane polarity cap, we imaged cells using the same growth conditions as above but without Sec15 induction (*GAL*-vector). This imaging revealed a fractional fluorescence of approximately 93 copies of Cdc42 per ROI. Since thin section electron micrographs of small budded yeast show an average of 1.3 ± 0.23 secretory vesicle in close proximity to the bud tip per section (per bud) or approximately 2.6 vesicles per 0.2 micron optical section, it was important to account for this contribution in our estimates. To accomplish this we subtracted the contribution of the 2.6 docked vesicles (~17 copies of Cdc42) from the total Cdc42 present in the ROI (93 copies) and divided the remaining amount (76 copies) by the plasma membrane surface area present in the ROI (0.094 μm^2). As shown in Figure 2.5G, this equates to a plasma membrane cap density of 810 copies of Cdc42 per square micron which is nearly three times the density of Cdc42 on the vesicle membrane (260 copies/μm^2).

To corroborate our findings described above, we also generated an estimate of the Cdc42 copy number by quantitative immunoblot analysis using an alternative reference standard, Sec1—a protein which the total copies per cell (determined by immunoblot) has previously been determined [68]. We generated a strain in which Sec1-GFP was integrated at the *SEC1* chromosomal locus such that it is expressed behind the native promoter and is the sole source Sec1 in the cell (see materials methods). Whole cell lysates of Sec1-GFP and GFP-Cdc42 expressing cells alongside an isogenic control strain were prepared, loaded by equivalent cell number and analyzed by Western blotting (Figure 2.5D). We applied the reported total copies of Sec1 (639 copies/cell) to the ratio of total GFP-Cdc42:Sec1-GFP and found the total copies of GFP-Cdc42 to be roughly 21,500. Using this copy number and the aforementioned comparative analyses of native Cdc42 protein levels under various conditions (see Figures 2.5B, C), we estimate ~5,400 copies of Cdc42 in polarized (uninduced) cells and ~8,200 copies of Cdc42 in cluster-forming (induced) cells. The compilation of the described data using both reference standards is reported in Figure 2.5G. Similar to our results using the Cse4 standard, we found the plasma membrane cap density of 636 Cdc42 copies per square micron to also be roughly three times the vesicle membrane density (204 copies/μm^2). Together these data suggest the immediate effect of post-Golgi vesicle fusion with the Cdc42 polarity cap would be to dilute rather than concentrate Cdc42 at the site of fusion. The implications of this surprising finding are discussed below.

2.4 Discussion

Delivery of Cdc42 by vesicle-mediated exocytic transport has been proposed to be an important mechanism by which Cdc42 polarity on the plasma membrane is both generated and maintained [57, 72]. In these models, Cdc42 associated with post-Golgi vesicles is delivered along actin cables to sites of polarized growth. The subsequent fusion of Cdc42-laden vesicles with the plasma membrane at these sites would promote Cdc42 polar cap formation. This would lead to a positive feedback loop by reinforcing the organization of actin cables oriented toward such sites, which in turn would bring more vesicles to this site [49, 57]. Another positive feedback loop could result from Cdc42's direct activation of the Exocyst tethering complex to promote its own polarization by increasing the rates of vesicle docking and fusion at specific sites of the plasma membrane –in a manner that is independent of actin [72, 73]. A critical assumption in both of these models is that the surface density of Cdc42 on post-Golgi vesicles must exceed the surface density at the plasma membrane polarity cap for polarity to be generated and/or maintained [50]. Mathematical modeling studies by Savage *et al*. [74], examined the theoretical effect of exocytic fusion of vesicles depleted of Cdc42 on the plasma membrane polarity cap. In their model such a situation perturbed local polarity in a manner that could be overcome in the presence of an active GDI recycling mechanism. The experimental data presented here demonstrate that such an effect is more than theoretical since the surface density we observe for Cdc42 on post Golgi vesicles is, in fact, roughly 3-fold more dilute than the density of Cdc42 we observe at the plasma membrane polarity cap. This indicates that the immediate effect of exocytic

vesicle fusion is to dilute the Cdc42 present at this site on the plasma membrane rather than to concentrate it, which is inconsistent with the actin-mediated positive feedback model [44, 57].

Since both the actin cytoskeleton and the vesicle docking/fusion apparatus are thought to direct traffic to sites on the plasma membrane with the most concentrated Cdc42, the local effect of exocytic transport would be to antagonize or destabilize Cdc42 polarization on the plasma membrane [56, 75]. Local negative regulation may play an important role in building spatial flexibility into this system. This is similar to a model recently proposed by Dyer *et al*. [76] in which dilution of the scaffolding protein Bem1 by vesicle fusion would lead to wandering of the polarity cap. Our data suggest that in addition to dilution of polarity factors such as Bem1, vesicle fusion would result in dilution of Cdc42 itself which would contribute directly to the destabilizing effect of exocytic transport on polarity.

If the immediate effect of exocytic traffic is to antagonize Cdc42 polarity on the plasma membrane, then why is Cdc42 associated with post-Golgi vesicles at all? While the work presented here does not directly address this important question, we can speculate on possible roles for exocytic delivery of Cdc42. First, exocytic delivery may represent a mechanism for recycling Cdc42 that has been removed by endocytosis [44, 45, 63]. Such a delivery system would fit with the notion that trafficking acts as a parallel pathway to the Rho GDI recycling mechanism as proposed by Slaughter *et al*. [44]. All of our data is in complete agreement with such a recycling function for vesicular Cdc42. Another function for this recycling mechanism is that having significant levels of Cdc42 on the vesicles helps to buffer

the negative regulatory effects of exocytic transport on Cdc42 polarity a possibility explored through modeling in the Savage *et al.* study [74].

A recent study examined the apparent surface densities of GFP-Cdc42 within the cell by fluorescence correlative spectroscopy [77]. In this paper, Slaughter *et al*. concluded that the surface density of GFP-Cdc42 on vesicles (49 molecules/μm^2) was similar to that on the plasma membrane (46 molecules/μm^2). The remarkably low absolute density reported at the polarity cap was particularly surprising given that such a density would involve a polarity cap (0.1μm^2) with only 4.3 GFP-Cdc42 molecules out of roughly 12,000 molecules per cell (based on a conservative estimate of the GFP-Cdc42/native Cdc42 expression levels for the GFP-Cdc42 constructs used) or less than 0.04% of the total cellular GFP-Cdc42. In contrast, our estimates of native Cdc42 densities on post-Golgi vesicles are almost 5-fold higher (260 molecules/μm^2 or 6.5 copies per vesicle) than Slaughter *et al*. (2013) and our estimates of densities on the plasma membrane (810 molecules/μm^2) are 15-fold higher. For comparison, our results indicate that a polarity cap (0.1μm^2) contains 76 molecules of native Cdc42 or roughly 1.1% of the total cellular Cdc42. Given the low densities of GFP-Cdc42 and the inferred low plasma membrane polarity reported by Slaughter *et al*. (2013) it is difficult to reconcile their findings with our work except to note that widely different approaches were used to estimate densities.

We also demonstrate that GFP-Cdc42 is defective in its association with post-Golgi vesicles compared to its untagged counterpart. Before the work presented in this paper, common methods were limited in the ability to quantitatively examine the amounts of the native, untagged Cdc42 protein associated with post-Golgi vesicles.

Thus, the inability to gather information on the native protein may have introduced gaps in our understanding that were not previously apparent. Both our data and Slaughter *et al*. [44] support the notion that Rdi1 and vesicle traffic act as parallel routes for Cdc42 cycling to and from the plasma membrane, which is somewhat surprising given the apparent recycling defect of GFP-Cdc42 compared to the untagged form [55, 66, 67]. Furthermore, it is interesting that GFP-Cdc42 supports growth of *rdi1*Δ *cdc42*Δ cells at temperatures below 30ºC (Figure 2.4D). This may indicate the existence of an additional or third recycling pathway that allows prenylated Cdc42 to be recycled between internal membranes and the plasma membrane polarity cap. Altogether, the data presented in this paper supports the importance of continued studies of the native protein alongside tagged forms of Cdc42 to improving our understanding of cell polarity.

2.5 Materials and Methods

Yeast strains, reagents and media

Yeast strains used and generated for this study are listed in Supplemental Table S1. Standard protocols for media, growth and genetic manipulations were used. Growth media used in this study includes: YPD (1% bacto-yeast extract, 2% bacto-peptone, 2% dextrose), S minimal (0.67% yeast nitrogen base without amino acids and 2% dextrose), and dropout media (0.67% yeast nitrogen base without amino acids, synthetic complete amino acid supplement minus appropriate amino acid(s)and 2% dextrose). Media components were obtained from US Biological (Swampscott, MA), Fisher Scientific (Pittsburgh, PA) and BD Biosciences (San Jose, CA). Galactose inductions involved growth in rich or minimal media with 3%

raffinose followed by 8-10 hour inductions with 1% galactose (US Biological, Swampscott, MA). Deletion mutants were generated by PCR amplification of either a KanMX or NatMX cassette using oligos designed against the –MX cassette and flanking DNA sequences of respective genes (e.g. *END4, PEP12,* etc.). The genomic DNA used as PCR template was extracted from deletion strains— developed by the Saccharomyces Genome Deletion Project— using standard protocol for genomic DNA extraction [78]. Yeast transformations of the –MX cassette into *GAL*-vector, -*SRO7* and –*SEC15* strains were performed using lithium acetate method [79]. G418 sulfate was obtained from US Biological. clonNAT (nourseothricin) was obtained from WERNER BioAgents (Jena, Germany). YIpLac211-*GFP-linker-CDC42* plasmid was received as a gift from the Lew laboratory (Duke University, Durham, NC). *GFP-linker-CDC42* (behind *CDC42* promoter) was subcloned into a *LEU2*, *CEN* vector (pRS315) and introduced into wild-type and the *CDC42*-plasmid shuffle strain. Zymolyase 100T, ampicillin, Hepes (free acid), and 5-fluoroorotic acid (5-FOA) were obtained from US Biological (Swampscott, MA). Sorbitol, β-mercaptoethanol, phenol, sodium azide, sodium fluoride, dithiothreitol (DTT), were obtained from Sigma Aldrich (St. Louis, MO). Chloroform, Terrific Broth, and dextrose were from Fisher Scientific (Pittsburgh, PA).

Subcellular fractionation

Wild-type and *sec6-4*$^{ts-}$ cells with or without *PEP12* or *RDI1* disruptions were grown in rich (YPD) media overnight at 25^{o}C to mid-log phase and shifted to 37^{o}C for 2hr to accumulate secretory vesicles. Approximately 200 OD_{599} units of cells were harvested and washed with 10ml of (10 mM Tris pH 7.5; 20mM NaN_3; 20mM

NaF) buffer. Cells were spheroplasted in 7.2ml of (100 mM Tris pH 7.5; 10 mM NaN_3; 1.2 M Sorbitol; 21 mM β-mercaptoethanol; 0.05mg/ml Zymolyase 100T) buffer for 30 min at 37°C and lysed in 6ml of ice-cold (10 mM triethanolamine, pH 7.2; 0.8M sorbitol; protease inhibitor cocktail: 2 µg/ml each of leupeptin, aprotinin, antipain; 20 µM pepstatin A; 2 mM 4-(2-aminoethyl)benzenesulfonyl fluoride) buffer. Lysed cells were centrifuged, cold at 450 x g for 4 min to remove unbroken cells. Cleared lysates were centrifuged in a Sorvall centrifuge (30,000 x g for 15 min at 4°C) to separate pellet and supernatant fractions. Supernatants were then centrifuged at 100,000 x g for 1hr at 4°C. Pellets were resuspended in lysis buffer at volumes equal to the supernatant fractions. Equal volumes of supernatant, pellet and total lysate fractions were boiled in SDS sample buffer and separated on a 12.5% SDS-polyacrylamide gel. Western blotting was performed using polyclonal α-Sso1/2 (1:2000), polyclonal α-Sec4 (1:1000) or monoclonal α-Cdc42 (1:200) antibodies. Quantitative Western analysis was performed with the Odyssey Infrared Imaging System (LI-COR Biosciences, Lincoln NE).

Plasmid shuffle assay

To determine whether *GFP-CDC42* can complement *cdc42*Δ in GDI-depleted cells, *CDC42* (*CEN*, *HIS*) or *GFP-linker-CDC42* (*CEN*, *HIS*) were transformed into *CDC42* plasmid shuffle strains that were either wild-type or disrupted for *RDI1*. Deletion of *RDI1* was accomplished by homologous recombination as described for the endocytic deletion mutants. After selection on sc-his plates, the original *CDC42* plasmid (*CEN, URA*) was evicted by growth on 5-FOA. Temperature sensitivity was evaluated at temperatures ranging from 14°C to 37.5°C. Images of higher

temperatures shown in Figure 2.4 represent phenotypic separation between the *RDI1* and *rdi1*Δ strains.

Immunofluorescence and fluorescence microscopy

Cells were grown to mid-log phase in 2% glucose media and shifted into 3% raffinose for 2/+ doublings. *GAL-SRO7* and -*SEC15* were induced by adding 1% galactose for 8-10 hours. Cells were fixed and processed for immunofluorescent staining as described previously [72, 80]. Double-labeled immunofluorescent staining of the plasma membrane polarity cap and post-Golgi vesicles was performed using ammonium sulfate precipitated, monoclonal mouse α-Sec4 (1:200) and affinity-purified, polyclonal rabbit α-Cdc42 (1:75) antibodies. For background correction, control staining was performed using rabbit and mouse IgG antibodies that lacked reactivity to any yeast protein. Secondary antibodies were Rhodamine Red-X-conjugated AffiniPure Goat Anti-Mouse IgG and Fluorescein Isothiocyanate (FITC)-conjugated AffiniPure Goat Anti-Rabbit IgG (Jackson ImmunoResearch Laboratories Inc., West Grove, PA), respectively. Secondary antibodies were used at 1:100-1:200 dilution. Single-plane immunofluorescent, GFP-fluorescent, and differential interference contrast (DIC) images were acquired using Nikon model E600 and 2D-deconvolved using MetaMorph software (Molecular Devices). Figures were prepared from deconvolved images using Adobe Photoshop and Illustrator (CS5.1).

Quantitative analysis of polarized and vesicle clustering cells

ImageJ [81] was used to conduct quantitative analysis of single plane, 2D-deconvolved images. Cdc42 fluorescence intensity (a.u.) was measured using

regions of interest (ROIs) drawn within the centroid, or peak intensity, of either the plasma membrane polarity cap or the post-Golgi vesicle cluster and throughout the cytoplasm of the respective cell. Increases in fluorescence intensities of Cdc42 associated with the polarity cap versus the cluster relative to the cytoplasm were calculated in Microsoft Excel. Data was presented as either 1) relative fluorescence: the ratio of the average fluorescence intensities of the Cdc42-positive compartment relative to the cytosol, 2) relative association: the Cdc42 compartment : cytosol ratio expressed as percent association relative to 100% wild-type, 3) phenotype penetrance: box and whisker plot of the Cdc42 compartment : cytosol ratio. Figures were prepared using Adobe Photoshop and Illustrator (CS5.1).

Ratio-metric analysis of GFP-Cdc42 using the Cse4 reference standard

Cells expressing either GFP-Cdc42 or Cse4-GFP were cultured at 25^{o}C in minimal media to mid-log phase. Equivalent OD_{599} of both strains were mixed and spread onto standard, uncoated microscope slides. Images were acquired as 400ms/frame, 24-frame Z-series, with 0.2μm step-size using an Olympus IX81 microscope. Additionally, cells were imaged using differential interference contrast alongside fluorescence acquisition to delineate cells. Image 3D deconvolution was performed using MetaMorph software (version 7.7.10.0; Molecular Devices) and sum-intensity projections and measurements using ImageJ [81]. Integrated fluorescence intensity and background correction for Cse4-GFP was obtained as described in Lawrimore *et al*. [71]. ROIs were drawn around the periphery of incipient and small-budded cells to obtain the total cellular integrated fluorescence intensity for GFP-Cdc42. Background corrections were obtained from whole cell

ROIs of controls cells that were imaged in mixture with GFP-Cdc42 expressing cells. Total copies of GFP-Cdc42 in the cell were calculated by: (average GFP-Cdc42 fluorescence intensity ÷ average Cse4-GFP fluorescence intensity) x 80 Cse4-GFP copies/cell (yielded ~27,400 copies/cell). Approximately 40 cells for each strain were measured.

Comparative analysis of Cdc42 protein

To compare the amounts of endogenous Cdc42 to the plasmid-derived tagged and untagged forms, quantitative Western analysis was performed using the Odyssey Infrared Imaging System (LI-COR Biosciences, Lincoln NE). Strains were grown overnight (25^{o}C) in minimal media to mid-log phase. Cells were then transferred to rich media for 2 doublings prior to harvesting 7 OD_{599} units for glass bead lysis. An aliquot of each of these cultures were diluted to 0.2-0.4 OD_{599} units and counted using a hemocytometer. Cells were then subjected to glass bead lysis and lysates boiled in SDS sample buffer. Lysates were normalized based on equivalent cell number, separated on an 11.5% polyacrylamide gel and analyzed by quantitative western blotting. The ratio of protein amounts of GFP-tagged to endogenous Cdc42 were applied to the total cellular copies of GFP-Cdc42 to determine the total cellular copies of the native, untagged protein (yielded ~6,800 copies/cell).

Quantitative Western blotting was also used to compare Cdc42 amounts in wild-type and vesicle clustering strains. Cells were cultured using the same growth conditions as for fluorescence imaging and loaded on a polyacrylamide gel based on

equivalent cell number. The ratio of protein amounts of wild-type and vesicle clustering strains yielded ~10,400 copies of Cdc42 in *GAL-SEC15* induced cells.

Ratio-metric analysis of GFP-Cdc42 using the Sec1 reference standard

To generate the reference standard strain, an EcoR1 linearized plasmid (pB1114) containing a N-terminal deletion of *SEC1* tagged with GFP was integrated into wild-type cells at the *SEC1* locus using standard yeast transformation method [79]. The resulting strain expresses *SEC1-GFP* as the sole copy in the cell. Cells expressing either GFP-Cdc42 or Sec1-GFP, as the sole source, were cultured and prepared for quantitative Western blotting as described for comparative analysis of Cdc42 protein (above). Western blotting was performed using monoclonal mouse α-GFP from Roche Diagnostics (Indianapolis, IN), polyclonal rabbit α-Adh1 (1:2000), or affinity purified polyclonal α-Exo70 (1:100) antibodies. The total copies of Sec1 per cell [68] was applied to the ratio of GFP-Cdc42:Sec1-GFP to obtain total cellular copies of GFP-Cdc42 (~21,500 copies/cell). The comparative analysis of plasmid-borne to native Cdc42, induced to uninduced cells was applied to determine the total native Cdc42 copies per cell in uninduced and induced cells, ~5,400 and 8,200 respectively.

Quantification of Cdc42 vesicle and polarity cap surface densities

GAL-induced vesicle clustering strains and the vector control strain were cultured and processed for immunofluorescence as previously described. Image acquisition for fixed samples was as follows: 800ms/frame, 14 to 18-frame Z-series, with 0.2μm step-size using an Olympus IX81 microscope. Image 3D deconvolution, sum-intensity projections and ROI measurements were performed to obtain the

integrated fluorescence of the entire cell (as described for GFP-Cdc42). Also from these deconvolved z-series, ROI scans for the polarity cap and vesicle cluster were performed on the z-plane with the peak Cdc42 integrated fluorescence signal. ROI diameters used for polarity cap (0.47μm) and vesicle cluster (0.72μm) were chosen based on size that consistently fit regions with homogeneous staining. The fractional amount of the total integrated fluorescence intensity for the polarity cap and cluster was determined and converted to copies per ROI using this work's estimates of the total copies of the native protein per cell. Approximately 50 cells per strain were used for this analysis.

Morphometric analysis of thin-section micrographs was performed to obtain surface densities of the polarity cap and vesicle cluster. Vesicle cluster analysis: vesicles were counted in six regions of known size in several thin-section micrographs yielding an average cluster packing density of 35.5 ± 3.9 vesicles/μm^2. A 0.2μm-thick z-plane can accommodate two vesicles with a 90nm diameter. With this two-vesicle maximum per optical section and an ROI area of 0.407μm^2, we estimate that each ROI used for immunofluorescence contains an average of 71 vesicles/ROI and a total vesicle membrane surface area of 0.72μm^2. Polarity cap analysis: small-budded wild-type cells from six independent EM fields were examined for the absence/presence of vesicles within the bud that were either associated with or adjacent to the plasma membrane. This analysis yielded an average of 1.3 ± 0.23 vesicles/μm^2 per thin-section or 2.6 vesicles/μm^2 per IF optical section. The resulting surface density was subtracted from the final polarity cap

density and the average copies per ROI, surface area and density for the polarity cap are reported alongside those for the vesicle cluster in Figure 2.5.

2.6 Figures

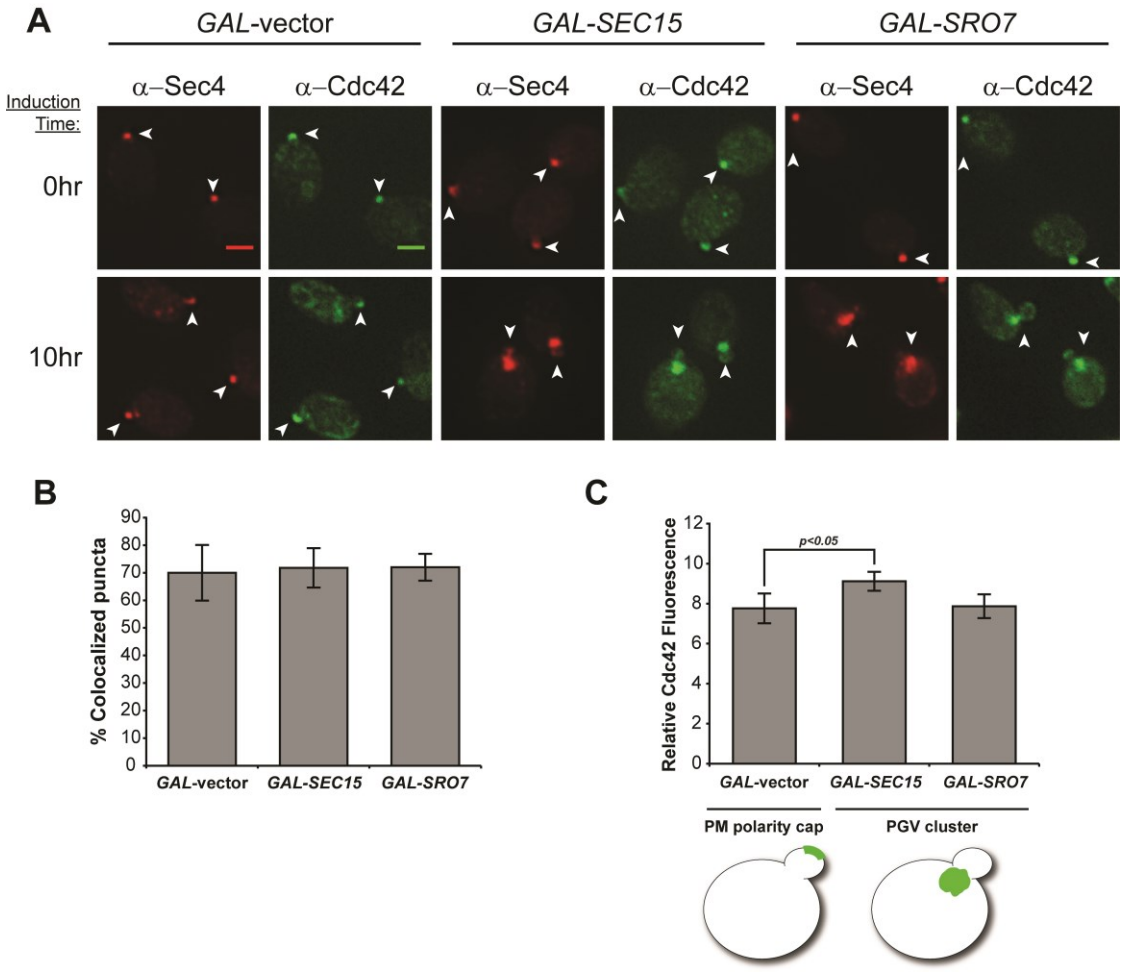

Figure 2.1 An *in vivo* assay demonstrates the association of Cdc42 with post-Golgi vesicles. A) Cdc42 localizes to Sec4+ post-Golgi vesicle clusters following *GAL*-overexpression of Sro7 and Sec15. Induced and uninduced cells were subjected to fixation and double-label immunofluorescence using monoclonal α-mouse Sec4 (red) and polyclonal α-rabbit Cdc42 (green) antibodies. Single-plane, 2D deconvolved images are shown. Cdc42/Sec4 co-staining for the plasma membrane polarity cap and post-Golgi vesicle clusters is denoted by arrowheads. Scale bar = 2μm. **B & C)** Quantitative analyses of Cdc42 association with Sec4+ compartments. **B)** Approximately 40 cells were selected based on Sec4+ staining and scored for Cdc42 co-localization. The bar graph compares the percentage of puncta showing co-localization in polarized and cluster-forming cells. Error bars represent standard deviation. **C)** The average ratio of Cdc42 at the polarity cap or vesicle clusters over the cytoplasm was measured (see Materials and Methods) in cells acquired from three independent experiments (approx. 140 cells). Error bars represent the standard deviation. Two-tailed Student *t* test was performed comparing vesicle clusters to the polarity cap (vector control). p=0.022

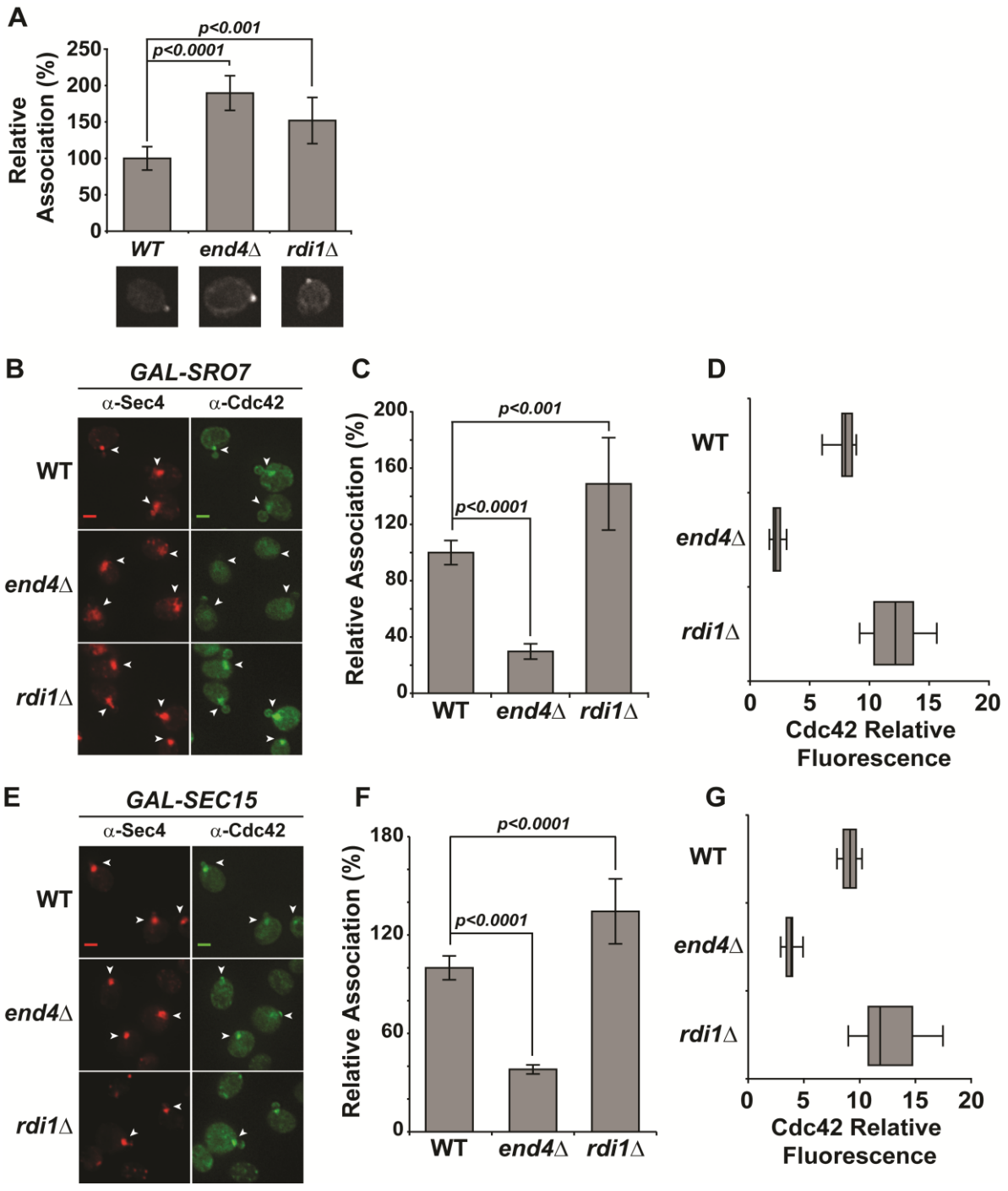

Figure 2.2 Endocytosis, but not Rho GDI, is required for Cdc42 association with post-Golgi vesicles. A) Cdc42 associates with the plasma membrane polarity cap in *RDI1*- and *END4* (*SLA2*)-depleted cells. Deletions in *RDI1* and *END4* were introduced into the *GAL-SRO7* vesicle clustering strain (see Materials and Methods). Cells were grown in raffinose media (25^{o}C) and subjected to IF as in Figure 2.1. The percent association of Cdc42 at the plasma membrane polarity cap in uninduced

wild-type, *rdi1*Δ and *end4*Δ cells were compared. Single-cell images represent the mean relative association; approx. 40 cells were scored; error bars represent the standard deviation. Two-tailed Student *t* test was performed to compare mutants to WT. **B-G)** Endocytic block impedes Cdc42 vesicle association**. B & E)** Galactose induction of vesicle clusters and IF staining was performed on wild-type, *rdi1*Δ, and *end4*Δ cells as described in Figure 2.1. Vesicle clusters are denoted by arrowheads. Scale bar = 2μm. **C & F)** Quantitative representation of the association of Cdc42 with Sro7- and Sec15-induced vesicle clusters (B & E respectively). The average Cdc42 fluorescence intensity was measured in cells randomly selected for Sec4+ vesicle clusters. Approximately 100 cells for each strain were scored. Error bars represent standard deviation. Data were normalized to percent association relative to 100% associated wild-type. Two-tailed Student *t* test was used to compare mutants to wild-type. **D & G)** Penetrance of *end4*Δ phenotype is shown as a box-and-whisker plot. The box represents the interquartile range (IQR) of the average relative Cdc42 fluorescence intensity. The line and whiskers denote the median and minimum/maximum, respectively.

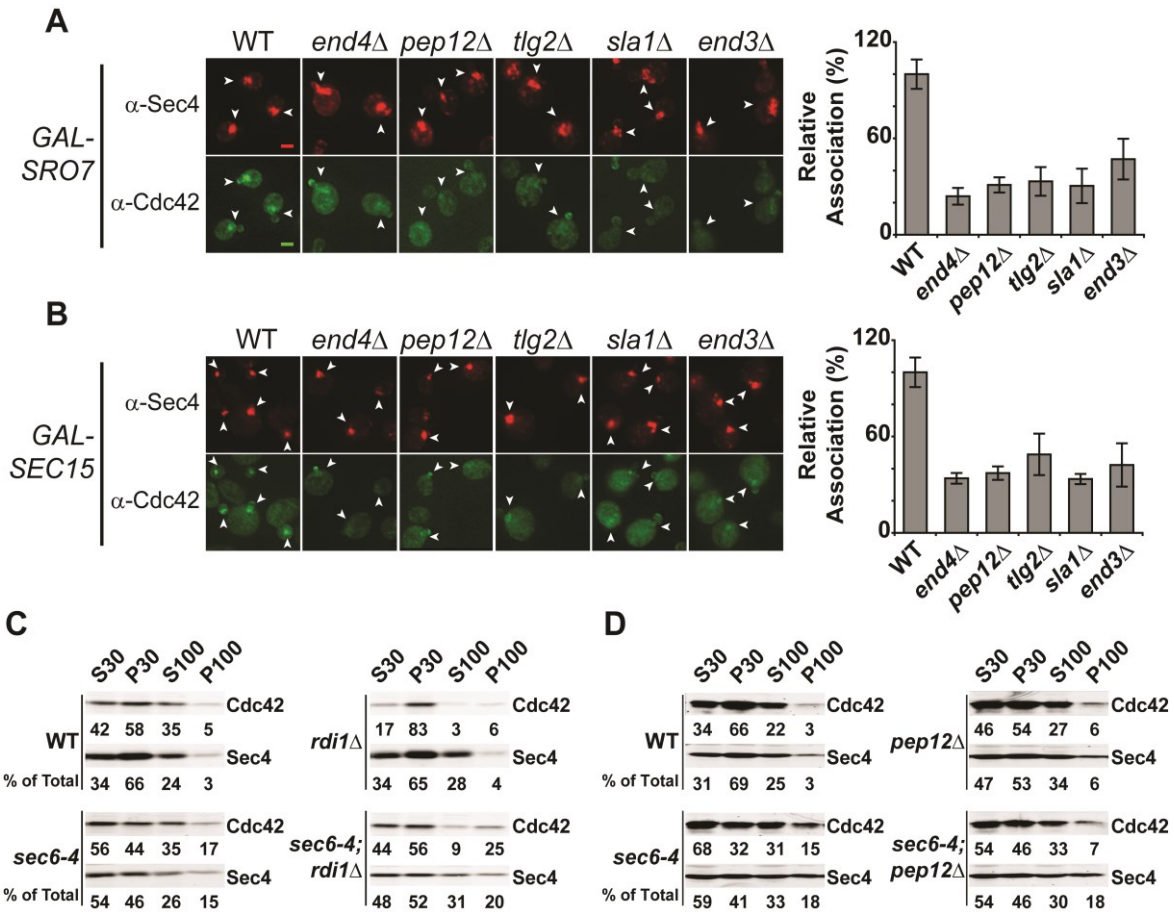

Figure 2.3 Endosomal sorting mutants show defects in Cdc42 recycling onto post-Golgi vesicles. A & B) Deletions in general endocytic regulators were introduced into the *GAL-SRO7* and –*SEC15* strains (see Materials and Methods). Cells were induced, fixed and subjected to IF as in Figure 2.2. Effect on Cdc42 vesicle cluster association is denoted by arrowheads. Data is presented as percent association relative to wild-type. Approximately 40 cells per strain were scored. Student *t* test was performed on all endocytic mutants compared to wild-type: A & B): all comparisons yielded $p<0.0001$. Scale bar = 2μm**. C & D)** Cdc42 associates with *sec6-4* derived post-Golgi vesicles in an endocytic-dependent, *RDI1*-independent manner. *PEP12* and *RDI1* disruptions were introduced into the late-secretory mutant *sec6-4* and an isogenic wild-type strain. Strains were grown in rich media overnight at 25°C to mid-log phase and shifted to 37°C for 2h to accumulate secretory vesicles. Cells were lysed and differential centrifugation was performed. Samples of low- and high-speed supernatants (S30 and S100) and pellets (P30 and P100) fractions were subjected to SDS-PAGE and Western analyses using antibodies against Sec4 and Cdc42 (see Materials and Methods). Percentages of total protein are shown under each blot.

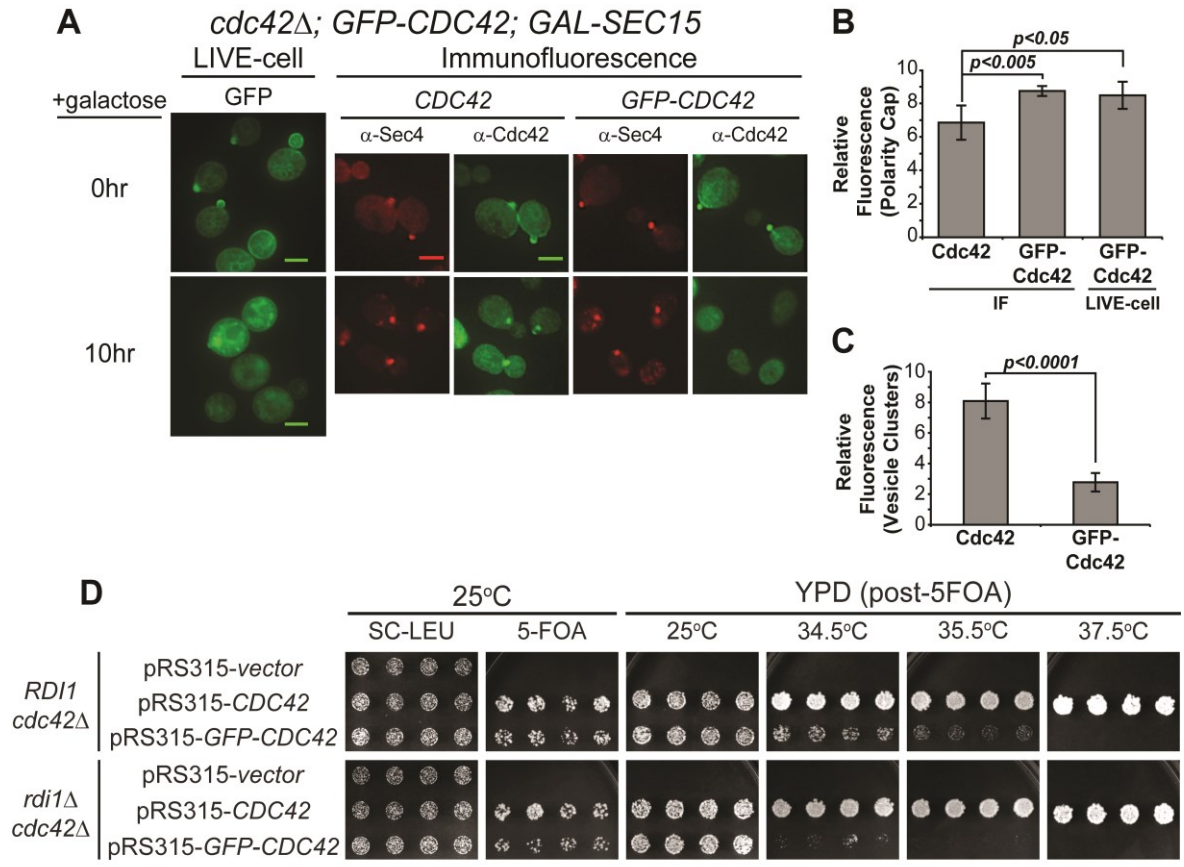

Figure 2.4 GFP-tagged Cdc42 has impaired ability to associate with post-Golgi vesicles and exhibits synthetic growth defects with *rdi1*Δ. A) GFP-Cdc42 does not accumulate under conditions that form Sec4+ post-Golgi vesicle clusters. Vesicles clusters were induced in cells that complement a *cdc42*Δ with either untagged or GFP-tagged *CDC42* expressed behind the *CDC42* promoter on a *LEU2/CEN* plasmid. Cdc42 vesicle and PM association was visualized by double-labeled IF of Sec4 and Cdc42. Live cell imaging of GFP-Cdc42 was performed before and after *GAL*-induction. **B & C)** Quantitative analysis of average relative GFP-Cdc42 fluorescence intensity at the PM (B, live-cell versus IF) and the cluster (C, IF only). Polarity cap (B): n = 25. Vesicle cluster (C): n = 50. Data comparing GFP-Cdc42 expressing cells to untagged Cdc42 (*CEN*) was analyzed by Student *t* test. (B) Comparison of Live, GFP-Cdc42 to native Cdc42 by IF: p=0.0235 Scale bar = 4μm **D)** *GFP-CDC42* is synthetically sick with *rdi1*Δ. Untagged or GFP-tagged *CDC42* were introduced into *CDC42*-plasmid shuffle strains that contained either *RDI1* or *rdi1*Δ. After selection on 5-FOA, growth on YPD was assessed at 25°C, 34.5°C, 35.5°C and 37.5°C.

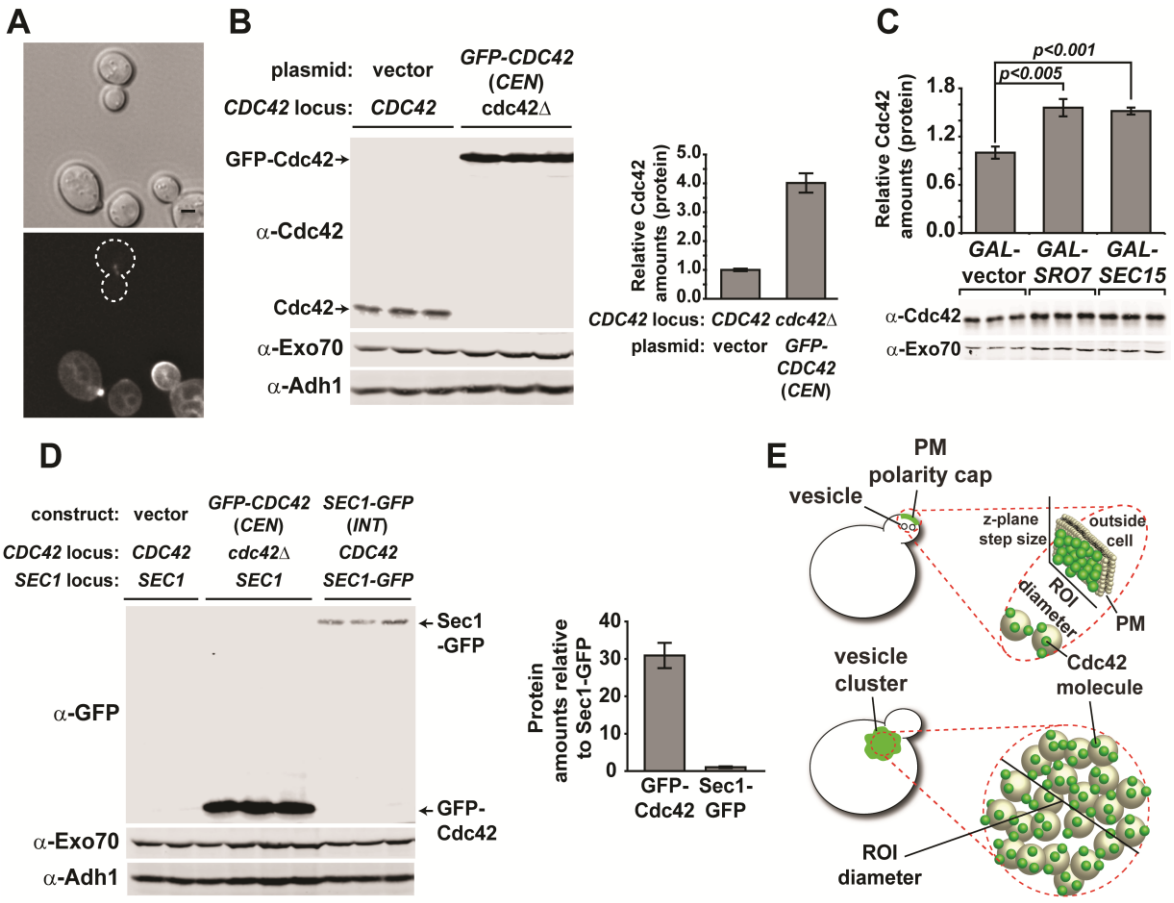

Patch Structure	PM Polarity Cap		Vesicle Cluster	
GAL-Sec15 conditions	Uninduced		Induced	
Reference Standard	CSE4	SEC1	CSE4	SEC1
ROI diameter (μm)	0.470		0.718	
Surface area (μm²/ROI)	0.094		0.723	
Average # vesicles/μm²	—		35.5 ± 3.9	
Cdc42 copies/vesicle	—		6.5	5.1
Total Cdc42 copies/cell	6846 ± 1091	5376 ± 494	10392 ± 295	8161 ± 231
Average copies/ROI	76.1 ± 6.4	59.8 ± 5.0	187.1 ± 19.7	146.9 ± 15.5
PM surface density (copies/μm²)	810 ± 67.6	636.1 ± 53.1	—	—
Vesicle surface density (copies/μm²)	—	—	259.9 ± 27.4	204 ± 21.5

Figure 2.5 Quantitative analysis of Cdc42 density on post-Golgi vesicles and the plasma membrane polarity cap. A) Fluorescence signal differences in GFP-Cdc42 and the reference standard, Cse4-GFP. Micrographs shown are sum-intensity projections from 24 deconvolved z-planes (bottom) and the reference

differential interference contrast (top). Scale bar = 2μm. **B)** Whole cell lysate comparison of cells expressing GFP-Cdc42 (*CEN*) or the chromosomal (untagged) Cdc42 in rich media. Protein samples were normalized by cell equivalents as described in Materials and Methods. Antibodies against Exo70 and Adh1 were used as loading controls. Quantification of the relative Cdc42 protein levels in GFP-Cdc42 expressing cells compared to cells expressing chromosomal Cdc42—when normalized by equivalent cell number. **C)** Whole celll lysate comparison of Cdc42 protein levels in vector, *GAL*-Sro7 and Sec15 after 8h induction in 1% galactose. Protein samples were loaded in duplicate based on equivalent cellular number. Exo70 was used as a loading control. Student *t* test was performed to compare relative Cdc42 amounts in clustering (*GAL*-Sro7 or –Sec15) versus non-clustering wild-type cells (vector). **D)** Whole cell lysate comparison of GFP-tagged Cdc42 (*CEN*) and Sec1-GFP (*INT*) in rich media. Protein samples were loaded in triplicate based on equivalent cell number. Western blotting was performed using monoclonal α-GFP and polyclonal α-Exo70 and α-Adh1 antibodies. Quantification of amounts of GFP-tagged protein relative to Sec1-GFP are shown. **E)** Schematic representation of measured surface densities associated with the polarity cap and vesicle cluster. **F)** Representative thin-section electron micrograph of vesicle cluster packing density. The thickness of each optical sections is 60nm. Scale bar = 2μm. **G)** Table of Cdc42 density estimates in polarity cap and vesicle cluster using Cse4 or Sec1 reference standards.

2.7 Supplementary Information

1. **Figure 2.S1**

2. **Table 2.S1**

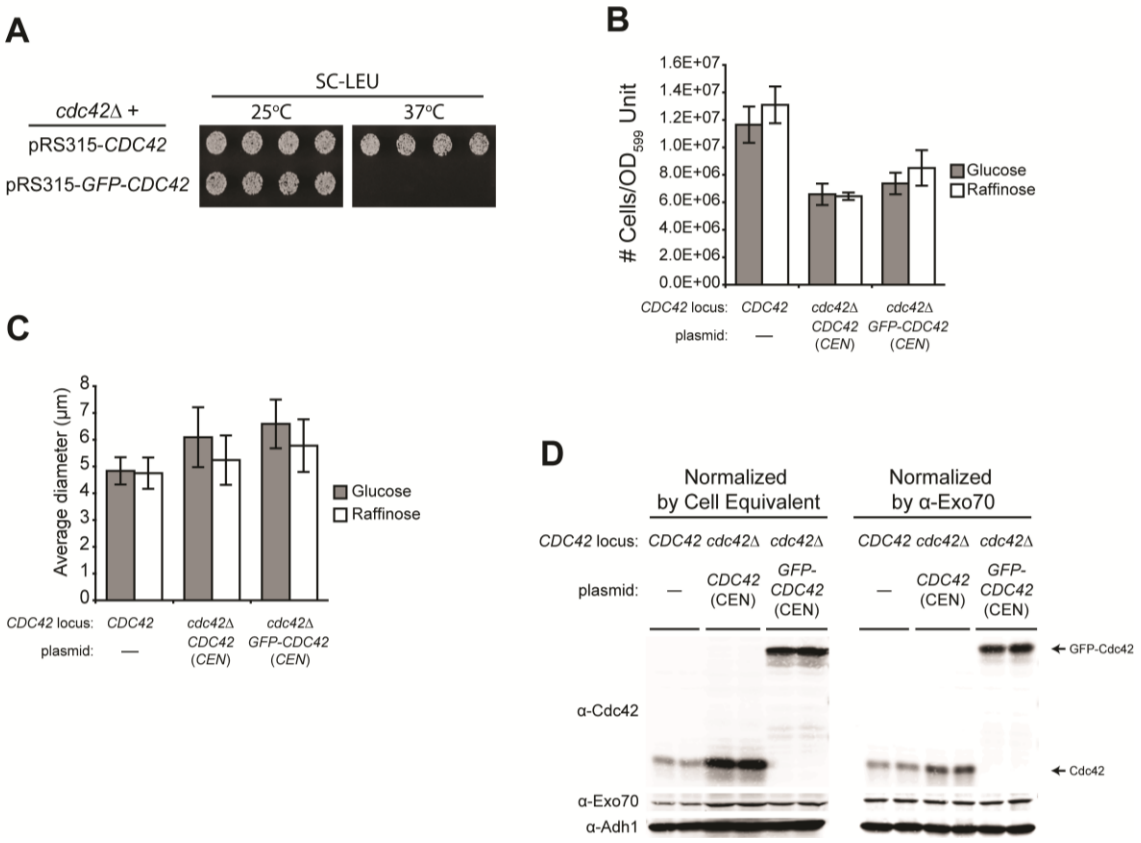

Figure 2.S1 Comparisons of strains containing untagged and GFP-tagged Cdc42. A) Expression of *GFP-CDC42* results in temperature sensitivity at 37°C. Plasmid-borne (*CEN*) GFP-tagged and untagged *CDC42* were introduced as the only source in the cell (see Experimental Procedures). These strains confirmed reported effects on growth at 37°C [55, 66, 67]. Four independent transformants for each strain were picked and transferred to minimal media at permissive (25°C) and non-permissive (37°C) temperatures. **B)** Effects of plasmid-borne (*CEN*) *CDC42* on OD_{599} equivalents. Cells with either native, untagged or GFP-tagged *CDC42* as the sole copy of Cdc42 were grown in either 2% glucose or 3% raffinose media to mid-log phase (2/+ doublings) at 25°C. The same number of OD_{599} were harvested, diluted to 0.2-0.7 OD_{599} and counted using a hemocytometer. Bar graphs show the average number of cells per OD_{599} Unit for each strain grown in both carbon sources. Error bars represent the standard deviation. Data were analyzed by two-tailed Student *t* test as compared to their respective wild-type control: all comparisons to wild-type yielded $p<0.0001$. **C)** Cells expressing

plasmid-derived *CDC42* show an increased cell diameter. Cells were grown as described in (B) and single plane, differential interference contrast (DIC) images were acquired using a Nikon model E600 microscope. Diameters of the mothers of budded cells were measured using ImageJ [81]. The average mother diameters of cells grown in glucose and raffinose are shown. Error bars represent the standard deviation; data were analyzed by two-tailed Student *t* test as compared to their respective wild-type control: all comparisons to control yielded $p<0.01$. **D)** Whole cell lysate comparison of native, untagged and GFP-tagged Cdc42 in 3% raffinose (minimal media). Left blot: samples were prepared and normalized to cell equivalents (as in Figure 2.5B). Right blot: samples were normalized by cell material (α-Exo70). Protein loading was monitored using α-Exo70 and α-Adh1 antibodies.

Table 2.S1: Yeast strains used in this study

Strain	MAT	Genotype	Reference
BY1807	a	*cdc42Δ::HIS3; pRS316-CDC42; ura3-52; leu2-3,112*	PB Collection
BY2368	α	*GAL+; LEU2::GAL-SRO7; ura3-52; leu2-3, 112; his3-Δ200*	[60]
BY2369	α	*GAL+; LEU2::GAL-SEC15; ura3-52; leu2-3, 112; his3-Δ200*	[60]
BY2375	α	*GAL+; LEU2::GAL-vector; ura3-52; leu2-3, 112; his3-Δ200*	[60]
BY2478	a	*ura3-52; leu2-3, 112*	PB Collection
BY2479	α	*rdi1Δ::KAN^r; ura3-52; leu2-3, 112*	PB Collection
BY2480	a	*sec6-4^{ts-}; ura3-52; leu2-3, 112*	PB Collection
BY2481	a	*sec6-4^{ts-}; rdi1Δ::KAN^r; ura3-52; leu2-3, 112*	PB Collection
BY2666	α	*GAL+; LEU2::GAL-SRO7; rdi1Δ::NAT^r; ura3-52; leu2-3, 112; his3-Δ200*	This study
BY2667	α	*GAL+; LEU2::GAL-SEC15; rdi1Δ::NAT^r; ura3-52; leu2-3, 112; his3-Δ200*	This study
BY2668	α	*GAL+; LEU2::GAL-vector; rdi1Δ::NAT^r; ura3-52; leu2-3, 112; his3-Δ200*	This study
BY2669	α	*GAL+; LEU2::GAL-SRO7; sla2Δ::KAN^r; ura3-52; leu2-3, 112; his3-Δ200*	This study
BY2670	α	*GAL+; LEU2::GAL-SEC15; sla2Δ::KAN^r; ura3-52; leu2-3, 112; his3-Δ200*	This study
BY2671	α	*GAL+; LEU2::GAL-vector; sla2Δ::KAN^r; ura3-52; leu2-3, 112; his3-Δ200*	This study
BY2685	α	*GAL+; LEU2::GAL-SRO7; pep12Δ::KAN^r; ura3-52; leu2-3, 112; his3-Δ200*	This study
BY2686	α	*GAL+; LEU2::GAL-SEC15; pep12Δ::KAN^r; ura3-52; leu2-3, 112; his3-Δ200*	This study

BY2687	α	*GAL+; LEU2::GAL-vector; pep12Δ::KAN^r; ura3-52; leu2-3, 112; his3-Δ200*	This study
BY2688	a	*pep12Δ::KAN^r; ura3-52; leu2-3, 112*	This study
BY2689	a	*sec6-4^{ts}; pep12Δ::KAN^r; ura3-52; leu2-3, 112*	This study
BY2707	α	*GAL+; LEU2::GAL-SRO7; tlg2Δ::KAN^r; ura3-52; leu2-3, 112; his3-Δ200*	This study
BY2708	α	*GAL+; LEU2::GAL-SEC15; tlg2Δ::KAN^r; ura3-52; leu2-3, 112; his3-Δ200*	This study
BY2709	α	*GAL+; LEU2::GAL-vector; tlg2Δ::KAN^r; ura3-52; leu2-3, 112; his3-Δ200*	This study
BY2710	α	*GAL+; LEU2::GAL-SRO7; sla1Δ::KAN^r; ura3-52; leu2-3, 112; his3-Δ200*	This study
BY2711	α	*GAL+; LEU2::GAL-SEC15; sla1Δ::KAN^r; ura3-52; leu2-3, 112; his3-Δ200*	This study
BY2712	α	*GAL+; LEU2::GAL-vector; sla1Δ::KAN^r; ura3-52; leu2-3, 112; his3-Δ200*	This study
BY2719	α	*GAL+; LEU2::GAL-SRO7; end3Δ::KAN^r; ura3-52; leu2-3, 112; his3-Δ200*	This study
BY2720	α	*GAL+; LEU2::GAL-SEC15; end3Δ::KAN^r; ura3-52; leu2-3, 112; his3-Δ200*	This study
BY2721	α	*GAL+; LEU2::GAL-vector; end3Δ::KAN^r; ura3-52; leu2-3, 112; his3-Δ200*	This study
BY3036	a	*cdc42Δ::HIS3; pRS315-CDC42; URA3::GAL-SEC15*	This study
BY3037	a	*cdc42Δ::HIS3; pRS315-GFP-CDC42; URA3::GAL-SEC15*	This study
BY3050	a	*cdc42Δ::HIS3; pRS316-CDC42; rdi1Δ::KAN^r; leu2-3,112*	This study
BY3152	α	*GAL+; SEC1-GFP::URA3; ura3-52; his3-Δ200*	This study
KBY2012	a	*cse4::HYG; pkk1; SPC29-CFP-KAN; trp1-63; leu2-1; ura3-52; his3-Δ200; lys2-801*	[82]

CHAPTER 3: Concluding Remarks and Future Studies

Maintenance of the polarized distribution of Cdc42 on the cell surface is dynamically achieved through the constant exchange of Cdc42 molecules between the polarity cap and internal pools [30, 44, 45]. Both the targeted delivery of proteins and lipids to the bud tip via exocytic transport and the diffusion of Cdc42 molecules away from the polarity cap can threaten the stability of the polarity cap. Recycling of Cdc42 from the plasma membrane presumably stabilizes the polarity cap by circumventing lateral membrane diffusion. Endocytic uptake and GDI-mediated retrieval of Cdc42 from the plasma membrane are considered parallel mechanisms for maintaining Cdc42's localization in this manner. Irazoqui *et al*. [45] demonstrated that endocytic recycling of Cdc42 counterbalances the targeted exocytic delivery of Cdc42-laden vesicles to the polarity cap suggesting that membrane trafficking serves to maintain the polarized localization of Cdc42. However, the feasibility of this concept of endo-exocytic trafficking of Cdc42 as a polarizing event is still quite controversial as it requires vesicles to deliver a significant amount of Cdc42 relative to the site on the plasma membrane to which the vesicles will ultimately fuse (Figure 1.3). As the amounts of native, untagged Cdc42 on vesicles compared to the polarity cap has yet to be determined, direct assessment of the vesicular contribution to Cdc42 polarity has been challenging. Therefore, the objective of my thesis has been to address this and other concerns of the role of endo-exocytic trafficking in maintaining the polarized localization of Cdc42.

First, using a novel phenotype that results in the accumulation of a pure population of Golgi-derived vesicles in the cytosol, we directly showed the enrichment of Cdc42 on secretory vesicles *in vivo*—which is consistent with previous biochemical studies conducted by other labs [46, 57, 58]. We also showed that deletions in genes that regulate distinct stages in the endocytic pathway disrupted the vesicle association of Cdc42, whereas loss of Rdi1 activity had no such effect in either the *in vivo* assay or biochemical fractionation assay (Figure 2.2 and 2.3). Removal of Cdc42 from the plasma membrane via endocytic recycling conceivably serves two functions. Firstly, given the potential for proteins that are peripherally associated with the plasma membrane to diffuse within the inner leaflet, endocytic uptake can serve to remove diffusing Cdc42 molecules from the plasma membrane. Additionally, the delivery and fusion of Cdc42-loaded exocytic vesicles with the polarity cap can potentially cause Cdc42 molecules to disperse around the plasma membrane depending on the vesicle concentration of Cdc42 (Figure 1.3) [50]. As endocytic patches are known to concentrate at sites adjacent to the polarity cap [83, 84], endocytic patches are perfectly positioned to counteract diffusion caused by vesicle fusion at or near the polarity cap. Secondly, like the role of endocytosis in the polarization of the v-SNARE Snc1 [85], endocytic recycling could serve to reload Cdc42 onto outward-bound secretory vesicles [45, 46]. As the association of Cdc42 with post-Golgi vesicles was largely dependent on its internalization and recycling via the endocytic pathway, not GDI-retrieval, our findings were consistent with these two roles of endocytosis in Cdc42 recycling. This differs from the plasma membrane polarity cap where both Rdi1 and membrane trafficking are considered to function in

parallel to regulate Cdc42's localization. Therefore, our findings also distinguished the requirements for vesicle recruitment from that involved in Cdc42's recruitment to the polarity cap.

Second, we provided the first direct estimation of the molecular distribution of native Cdc42 on post-Golgi vesicles compared to the polarity cap. Previous analyses of the contribution of membrane trafficking to Cdc42 polarity have involved mathematical modeling or fluorescence correlative spectroscopy of GFP-tagged Cdc42 [50, 77]. However, direct validation (or invalidation) of membrane trafficking as a polarizing agent required having precise estimations of the concentration of native Cdc42 on post-Golgi vesicles and the plasma membrane polarity cap. Using two independent methods, we found that while the amounts of native Cdc42 on vesicles is substantial in comparison to the surrounding cytosol, the concentration of Cdc42 at the polarity cap exceeded the vesicular concentration by threefold. Recent mathematical modeling studies suggests that fusion of secretory vesicles with the plasma membrane could result in dispersal of the polarity cap [50]. We demonstrated that the concentration of Cdc42 on post-Golgi vesicles is not sufficient to reinforce the polarized localization of Cdc42, and thus we provided the first experimental evidence for a negative role for membrane trafficking on Cdc42 polarity.

Third, we demonstrated that the addition of a GFP-tag to the N-terminus of Cdc42 impairs its ability to associate with post-Golgi vesicles. The importance of the C-terminus to Rho protein function and localization has been well documented [29, 31, 35, 53]. However, earlier work from our lab implicated the N-terminus in the

proper localization and function of Cdc42 and another Rho GTPase Rho3. Exchanging the N-termini of these two proteins resulted in loss of Rho3 localization and function, while the chimeric Cdc42 protein adopted a “Rho3-like” localization and ability to function as the sole source of Rho3 in the cell. The impaired association of the N-terminally tagged GFP-Cdc42 with post-Golgi vesicles presented in this thesis further demonstrated the significance of the extreme N-terminus in Cdc42’s localization. GFP-tagged forms of *CDC42* have been shown to have a growth defect at higher temperatures when serving as the only copy of *CDC42* in the cell (Figure S2.1) [55, 66, 67]. We found that the additional loss of *RDI1* function further diminishes the ability of *GFP-CDC42* to function as the sole source of *CDC42* in the cell, which suggests GFP-Cdc42 has a recycling defect. While the worsening of the temperature sensitivity of *GFP-CDC42* in *RDI1*-depleted cells was consistent with the parallel function of endocytosis and Rdi1, the ability of *GFP-CDC42* to support growth at ambient temperatures suggested the possibility of a third independent mechanism for recycling Cdc42 from the polarity cap. Altogether, these findings suggested that although studies using GFP-Cdc42 have contributed extensively to our understanding the polarization of Cdc42, tagging Cdc42 at the N-terminus could obscure the detection of additional mechanisms involved in Cdc42’s localization and its function in polarized growth.

Although the work described herein is in agreement with the proposed parallel function of membrane trafficking and GDI-mediated retrieval in recycling Cdc42 from the plasma membrane polarity cap, the dilute molecular distribution of Cdc42 on vesicles compared to the polarity cap suggests membrane trafficking serves to

antagonize rather than promote Cdc42 polarity (Figure 3.1). The antagonistic effect is consistent with the role of negative feedback systems in supporting spatial and temporal flexibility in responses to external/internal stimuli—such as that proposed for patch wandering during chemical gradient detection or in patch competition during the establishment of a single cell "front" [67, 76]. However, the direct trafficking of Cdc42-laden vesicles to the polarity cap—which is the site on the cell surface with the most concentrated Cdc42 distribution—could promote septin ring formation which in turn would serve as a barrier to restrict Cdc42 molecules to the polarity cap thereby preventing lateral membrane diffusion of Cdc42 [75].

3.1 Future Studies

The work presented in this thesis has provided several insights into the role of membrane trafficking in Cdc42 polarity. However, several unanswered questions remain. We found that Cdc42's association with post-Golgi secretory vesicles heavily depended on a functional endocytic pathway. Selective endocytic uptake of cell surface proteins has been shown to be involved in the stabilization of plasma membrane localization [85-89]. This may involve clathrin-mediated enrichment of cell surface proteins at sites of endocytosis followed by trafficking through endosomal and Golgi compartments to be redelivered to the plasma membrane as post-Golgi vesicle cargo [85]. As the disruption of endocytic genes known to regulate internalization (i.e. *END4* and *SLA1*) severely disrupted the ability of Cdc42 to localize to post-Golgi vesicles (Figure 2.3), our data is consistent with the possibility of the recruitment and enrichment of Cdc42 at sites of endocytosis and begs an important question as to the existence of a specific clathrin adaptor for Cdc42

uptake. There are many functional redundancies within the yeast genome that could obscure the identification of such an adaptor. Therefore, the identification of a Cdc42-specific adaptor may require large screens of potential candidates and/or the development of high-throughput assays.

Exchanging the N-terminal sequences of Rho3 and Cdc42 was previously shown by our lab to cause Cdc42 to adopt a dispersed “Rho3-like” localization pattern and function [37]. Work in this thesis revealed a significant reduction in Cdc42’s ability to be recycled onto post-Golgi secretory vesicles when a GFP-tag was placed on its N-terminus (Figure 2.4). Together with the requirement for endocytic recycling in Cdc42’s association with secretory vesicles, these observations evoke the possibility of a recycling element within the N-terminus of Cdc42 and the importance of this region in Cdc42’s recruitment to sites of endocytosis prior to internalization. The endocytic uptake of the alpha receptor Ste2 depends on the Sla1/End4/End3 pathway and an internalization signal located within its cytoplasmic tail [64, 90, 91]. The involvement of the Sla1/End4/End3 pathway in Cdc42’s recycling onto secretory vesicles suggests the possibility of an internalization signal. However, as the N-terminus contains both GTP-binding and effector-binding domains, it is also possible that this region could facilitate internalization through protein-protein interactions (i.e. through an adaptor or effector molecule). As Cdc42 is not known to possess a clear internalization signal and its internalization has yet to be shown to require any protein-protein interaction, the mechanism(s) involved in the recruitment and enrichment of Cdc42 to sites of endocytosis remains undefined. Therefore, future studies should focus on further

characterizing the N-terminus and/or other regions of Cdc42 for the possible involvement in the endocytic uptake of Cdc42.

We also found that although the concentration of Cdc42 on post-Golgi vesicles was insufficient to independently maintain Cdc42's polarized localization, the concentration on vesicles was still quite significant (Figure 2.5). Why load secretory vesicles with any amount of Cdc42 at all? A simple answer would be that fusion of "naked" vesicles would cause the polarity cap to rapidly disperse and overall polarity to collapse. However, as Cdc42 is known to manage polarity pathways independent from one another to coordinate cell polarity [92-94], having significant concentrations of Cdc42 on vesicles compared to the surrounding cytosol could play a role in Cdc42's specific regulation of polarized exocytosis—maybe through its recruitment of Exocyst subunits to vesicles or the plasma membrane. While this is highly speculative, future studies should be directed towards understanding how different levels of Cdc42 on vesicles could affect the proper localization of its effectors.

One function of GDI is to extract GDP-Cdc42 from membranes [15, 33]. The data presented in this thesis supports the idea that GDI-mediated retrieval and endocytic uptake of Cdc42 act in parallel to recycle Cdc42 from the plasma membrane polarity cap. However, it has yet to be determined whether endocytic recycling truly acts in parallel to selectively recycle inactive, GDP-Cdc42 from the plasma membrane. Future studies focused on these and other questions will significantly contribute to the elucidation of the precise role for membrane trafficking in Cdc42 polarity.

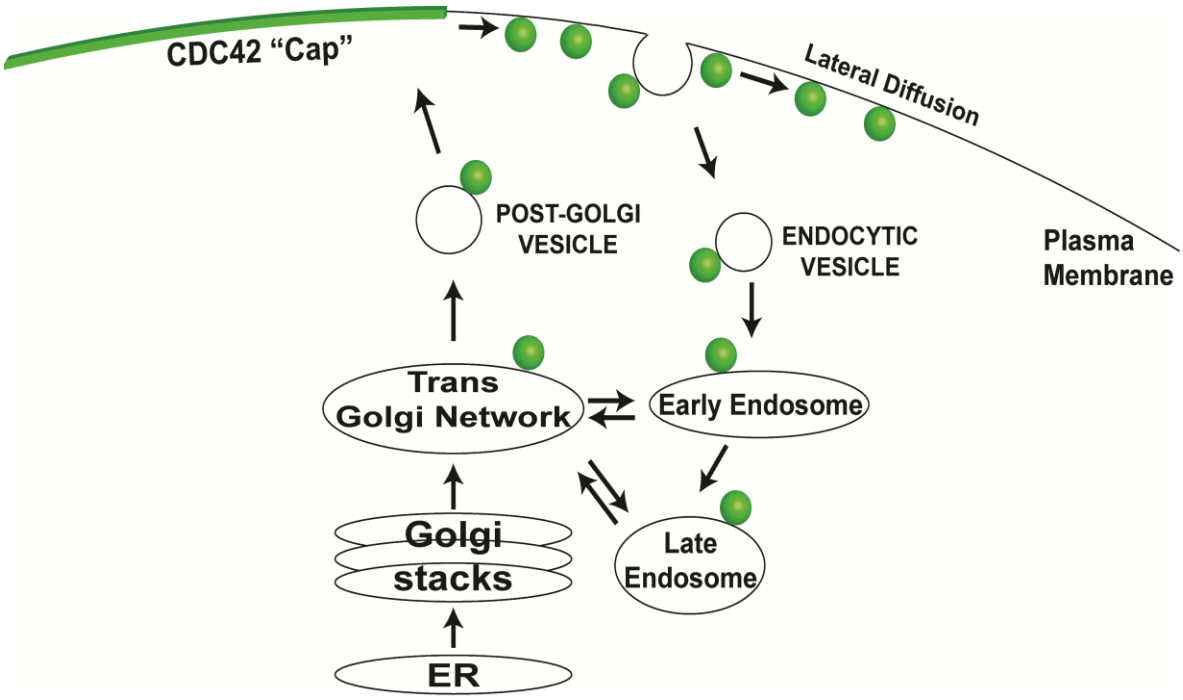

Figure 3.1 Schematic representation of the consequence of exocytic delivery on Cdc42 polarity. Endocytic uptake of Cdc42 from the concentrated polarity cap serves to recycle Cdc42 onto post-Golgi secretory vesicles for redelivery to the plasma membrane polarity cap. However, because the concentration of Cdc42 on post-Golgi vesicles is significantly lower than the polarity cap, the immediate effect of delivery and fusion of post-Golgi vesicles is to dilute the polarity cap.

REFERENCES

1. Drubin, D.G., and Nelson, W.J. (1996). Origins of cell polarity. Cell *84*, 335-344.

2. Chant, J. (1999). Cell polarity in yeast. Annual review of cell and developmental biology *15*, 365-391.

3. Vega-Salas, D.E., Salas, P.J., Gundersen, D., and Rodriguez-Boulan, E. (1987). Formation of the apical pole of epithelial (Madin-Darby canine kidney) cells: polarity of an apical protein is independent of tight junctions while segregation of a basolateral marker requires cell-cell interactions. J Cell Biol *104*, 905-916.

4. Manes, S., Mira, E., Gomez-Mouton, C., Lacalle, R.A., Keller, P., Labrador, J.P., and Martinez, A.C. (1999). Membrane raft microdomains mediate front-rear polarity in migrating cells. EMBO J *18*, 6211-6220.

5. Johnson, J.M., Jin, M., and Lew, D.J. (2011). Symmetry breaking and the establishment of cell polarity in budding yeast. Curr Opin Genet Dev *21*, 740-746.

6. Imai, J., Toh-e, A., and Matsui, Y. (1996). Genetic analysis of the Saccharomyces cerevisiae RHO3 gene, encoding a rho-type small GTPase, provides evidence for a role in bud formation. Genetics *142*, 359-369.

7. Matsui, Y., and Toh, E.A. (1992). Yeast RHO3 and RHO4 ras superfamily genes are necessary for bud growth, and their defect is suppressed by a high dose of bud formation genes CDC42 and BEM1. Mol Cell Biol *12*, 5690-5699.

8. Yamochi, W., Tanaka, K., Nonaka, H., Maeda, A., Musha, T., and Takai, Y. (1994). Growth site localization of Rho1 small GTP-binding protein and its involvement in bud formation in Saccharomyces cerevisiae. J Cell Biol *125*, 1077-1093.

9. Adams, A.E., Johnson, D.I., Longnecker, R.M., Sloat, B.F., and Pringle, J.R. (1990). CDC42 and CDC43, two additional genes involved in budding and the establishment of cell polarity in the yeast Saccharomyces cerevisiae. J Cell Biol *111*, 131-142.

10. Johnson, D.I., and Pringle, J.R. (1990). Molecular characterization of CDC42, a Saccharomyces cerevisiae gene involved in the development of cell polarity. J Cell Biol *111*, 143-152.

11. Vega, F.M., and Ridley, A.J. (2008). Rho GTPases in cancer cell biology. FEBS Lett *582*, 2093-2101.

12. Johnson, D.I. (1999). Cdc42: An essential Rho-type GTPase controlling eukaryotic cell polarity. Microbiol Mol Biol Rev *63*, 54-105.

13. Bender, A., and Pringle, J.R. (1989). Multicopy suppression of the cdc24 budding defect in yeast by CDC42 and three newly identified genes including the ras-related gene RSR1. Proc Natl Acad Sci U S A *86*, 9976-9980.

14. Howell, A.S., and Lew, D.J. (2012). Morphogenesis and the cell cycle. Genetics *190*, 51-77.

15. Bi, E., and Park, H.O. (2012). Cell polarization and cytokinesis in budding yeast. Genetics *191*, 347-387.

16. Sherman, F. (2002). Getting started with yeast. Methods Enzymol *350*, 3-41.

17. Chant, J., and Herskowitz, I. (1991). Genetic control of bud site selection in yeast by a set of gene products that constitute a morphogenetic pathway. Cell *65*, 1203-1212.

18. Fujita, A., Oka, C., Arikawa, Y., Katagai, T., Tonouchi, A., Kuhara, S., and Misumi, Y. (1994). A yeast gene necessary for bud-site selection encodes a protein similar to insulin-degrading enzymes. Nature *372*, 567-570.

19. Zahner, J.E., Harkins, H.A., and Pringle, J.R. (1996). Genetic analysis of the bipolar pattern of bud site selection in the yeast Saccharomyces cerevisiae. Mol Cell Biol *16*, 1857-1870.

20. Chant, J., Corrado, K., Pringle, J.R., and Herskowitz, I. (1991). Yeast BUD5, encoding a putative GDP-GTP exchange factor, is necessary for bud site selection and interacts with bud formation gene BEM1. Cell *65*, 1213-1224.

21. Chant, J., and Pringle, J.R. (1991). Budding and cell polarity in Saccharomyces cerevisiae. Curr Opin Genet Dev *1*, 342-350.

22. Etienne-Manneville, S. (2004). Cdc42--the centre of polarity. J Cell Sci *117*, 1291-1300.

23. Hartwell, L.H., Mortimer, R.K., Culotti, J., and Culotti, M. (1973). Genetic Control of the Cell Division Cycle in Yeast: V. Genetic Analysis of cdc Mutants. Genetics *74*, 267-286.

24. Sloat, B.F., Adams, A., and Pringle, J.R. (1981). Roles of the CDC24 gene product in cellular morphogenesis during the Saccharomyces cerevisiae cell cycle. J Cell Biol *89*, 395-405.

25. Miller, P.J., and Johnson, D.I. (1994). Cdc42p GTPase is involved in controlling polarized cell growth in Schizosaccharomyces pombe. Mol Cell Biol *14*, 1075-1083.

26. Shinjo, K., Koland, J.G., Hart, M.J., Narasimhan, V., Johnson, D.I., Evans, T., and Cerione, R.A. (1990). Molecular cloning of the gene for the human placental GTP-binding protein Gp (G25K): identification of this GTP-binding protein as the human homolog of the yeast cell-division-cycle protein CDC42. Proc Natl Acad Sci U S A *87*, 9853-9857.

27. Chen, F., Ma, L., Parrini, M.C., Mao, X., Lopez, M., Wu, C., Marks, P.W., Davidson, L., Kwiatkowski, D.J., Kirchhausen, T., et al. (2000). Cdc42 is required for PIP(2)-induced actin polymerization and early development but not for cell viability. Curr Biol *10*, 758-765.

28. Martin, S.G., and Arkowitz, R.A. (2014). Cell polarization in budding and fission yeasts. FEMS microbiology reviews *38*, 228-253.

29. Richman, T.J., Sawyer, M.M., and Johnson, D.I. (2002). Saccharomyces cerevisiae Cdc42p localizes to cellular membranes and clusters at sites of polarized growth. Eukaryot Cell *1*, 458-468.

30. Wedlich-Soldner, R., Wai, S.C., Schmidt, T., and Li, R. (2004). Robust cell polarity is a dynamic state established by coupling transport and GTPase signaling. J Cell Biol *166*, 889-900.

31. Ziman, M., O'Brien, J.M., Ouellette, L.A., Church, W.R., and Johnson, D.I. (1991). Mutational analysis of CDC42Sc, a Saccharomyces cerevisiae gene that encodes a putative GTP-binding protein involved in the control of cell polarity. Mol Cell Biol *11*, 3537-3544.

32. Caviston, J.P., Tcheperegine, S.E., and Bi, E. (2002). Singularity in budding: a role for the evolutionarily conserved small GTPase Cdc42p. Proc Natl Acad Sci U S A *99*, 12185-12190.

33. Eitzen, G., Thorngren, N., and Wickner, W. (2001). Rho1p and Cdc42p act after Ypt7p to regulate vacuole docking. EMBO J *20*, 5650-5656.

34. Masuda, T., Tanaka, K., Nonaka, H., Yamochi, W., Maeda, A., and Takai, Y. (1994). Molecular cloning and characterization of yeast rho GDP dissociation inhibitor. J Biol Chem *269*, 19713-19718.

35. Richman, T.J., Toenjes, K.A., Morales, S.E., Cole, K.C., Wasserman, B.T., Taylor, C.M., Koster, J.A., Whelihan, M.F., and Johnson, D.I. (2004). Analysis of cell-cycle specific localization of the Rdi1p RhoGDI and the structural determinants required for Cdc42p membrane localization and clustering at sites of polarized growth. Current genetics *45*, 339-349.

36. Tcheperegine, S.E., Gao, X.D., and Bi, E. (2005). Regulation of cell polarity by interactions of Msb3 and Msb4 with Cdc42 and polarisome components. Mol Cell Biol *25*, 8567-8580.

37. Wu, H., and Brennwald, P. (2010). The function of two Rho family GTPases is determined by distinct patterns of cell surface localization. Mol Cell Biol *30*, 5207-5217.

38. Butty, A.C., Perrinjaquet, N., Petit, A., Jaquenoud, M., Segall, J.E., Hofmann, K., Zwahlen, C., and Peter, M. (2002). A positive feedback loop stabilizes the guanine-nucleotide exchange factor Cdc24 at sites of polarization. EMBO J *21*, 1565-1576.

39. Howell, A.S., Savage, N.S., Johnson, S.A., Bose, I., Wagner, A.W., Zyla, T.R., Nijhout, H.F., Reed, M.C., Goryachev, A.B., and Lew, D.J. (2009). Singularity in polarization: rewiring yeast cells to make two buds. Cell *139*, 731-743.

40. Irazoqui, J.E., Gladfelter, A.S., and Lew, D.J. (2003). Scaffold-mediated symmetry breaking by Cdc42p. Nat Cell Biol *5*, 1062-1070.

41. Kozubowski, L., Saito, K., Johnson, J.M., Howell, A.S., Zyla, T.R., and Lew, D.J. (2008). Symmetry-breaking polarization driven by a Cdc42p GEF-PAK complex. Curr Biol *18*, 1719-1726.

42. Chen, H., Kuo, C.C., Kang, H., Howell, A.S., Zyla, T.R., Jin, M., and Lew, D.J. (2012). Cdc42p regulation of the yeast formin Bni1p mediated by the effector Gic2p. Mol Biol Cell *23*, 3814-3826.

43. Dong, Y., Pruyne, D., and Bretscher, A. (2003). Formin-dependent actin assembly is regulated by distinct modes of Rho signaling in yeast. J Cell Biol *161*, 1081-1092.

44. Slaughter, B.D., Das, A., Schwartz, J.W., Rubinstein, B., and Li, R. (2009). Dual modes of Cdc42 recycling fine-tune polarized morphogenesis. Dev Cell *17*, 823-835.

45. Irazoqui, J.E., Howell, A.S., Theesfeld, C.L., and Lew, D.J. (2005). Opposing roles for actin in Cdc42p polarization. Mol Biol Cell *16*, 1296-1304.

46. Orlando, K., Sun, X., Zhang, J., Lu, T., Yokomizo, L., Wang, P., and Guo, W. (2011). Exo-endocytic trafficking and the septin-based diffusion barrier are required for the maintenance of Cdc42p polarization during budding yeast asymmetric growth. Mol Biol Cell *22*, 624-633.

47. Boulter, E., Garcia-Mata, R., Guilluy, C., Dubash, A., Rossi, G., Brennwald, P.J., and Burridge, K. (2010). Regulation of Rho GTPase crosstalk, degradation and activity by RhoGDI1. Nat Cell Biol *12*, 477-483.

48. Tiedje, C., Sakwa, I., Just, U., and Hofken, T. (2008). The Rho GDI Rdi1 regulates Rho GTPases by distinct mechanisms. Mol Biol Cell *19*, 2885-2896.

49. Slaughter, B.D., Smith, S.E., and Li, R. (2009). Symmetry breaking in the life cycle of the budding yeast. Cold Spring Harb Perspect Biol *1*, a003384.

50. Layton, A.T., Savage, N.S., Howell, A.S., Carroll, S.Y., Drubin, D.G., and Lew, D.J. (2011). Modeling vesicle traffic reveals unexpected consequences for Cdc42p-mediated polarity establishment. Curr Biol *21*, 184-194.

51. Brennwald, P., and Rossi, G. (2007). Spatial regulation of exocytosis and cell polarity: yeast as a model for animal cells. FEBS Lett *581*, 2119-2124.

52. Park, H.O., and Bi, E. (2007). Central roles of small GTPases in the development of cell polarity in yeast and beyond. Microbiol Mol Biol Rev *71*, 48-96.

53. Ziman, M., Preuss, D., Mulholland, J., O'Brien, J.M., Botstein, D., and Johnson, D.I. (1993). Subcellular localization of Cdc42p, a Saccharomyces cerevisiae GTP-binding protein involved in the control of cell polarity. Mol Biol Cell *4*, 1307-1316.

54. Ozbudak, E.M., Becskei, A., and van Oudenaarden, A. (2005). A system of counteracting feedback loops regulates Cdc42p activity during spontaneous cell polarization. Dev Cell *9*, 565-571.

55. Freisinger, T., Klunder, B., Johnson, J., Muller, N., Pichler, G., Beck, G., Costanzo, M., Boone, C., Cerione, R.A., Frey, E., et al. (2013). Establishment of a robust single axis of cell polarity by coupling multiple positive feedback loops. Nat Commun *4*, 1807.

56. Jose, M., Tollis, S., Nair, D., Sibarita, J.B., and McCusker, D. (2013). Robust polarity establishment occurs via an endocytosis-based cortical corralling mechanism. J Cell Biol *200*, 407-418.

57. Wedlich-Soldner, R., Altschuler, S., Wu, L., and Li, R. (2003). Spontaneous cell polarization through actomyosin-based delivery of the Cdc42 GTPase. Science *299*, 1231-1235.

58. Forsmark, A., Rossi, G., Wadskog, I., Brennwald, P., Warringer, J., and Adler, L. (2011). Quantitative proteomics of yeast post-Golgi vesicles reveals a discriminating role for Sro7p in protein secretion. Traffic *12*, 740-753.

59. Salminen, A., and Novick, P.J. (1989). The Sec15 protein responds to the function of the GTP binding protein, Sec4, to control vesicular traffic in yeast. J Cell Biol *109*, 1023-1036.

60. Rossi, G., and Brennwald, P. (2011). Yeast homologues of lethal giant larvae and type V myosin cooperate in the regulation of Rab-dependent vesicle clustering and polarized exocytosis. Mol Biol Cell *22*, 842-857.

61. Guo, W., Roth, D., Walch-Solimena, C., and Novick, P. (1999). The exocyst is an effector for Sec4p, targeting secretory vesicles to sites of exocytosis. EMBO J *18*, 1071-1080.

62. Pfeffer, S.R., Dirac-Svejstrup, A.B., and Soldati, T. (1995). Rab GDP dissociation inhibitor: putting rab GTPases in the right place. J Biol Chem *270*, 17057-17059.

63. Yamamoto, T., Mochida, J., Kadota, J., Takeda, M., Bi, E., and Tanaka, K. (2010). Initial polarized bud growth by endocytic recycling in the absence of actin cable-dependent vesicle transport in yeast. Mol Biol Cell *21*, 1237-1252.

64. Raths, S., Rohrer, J., Crausaz, F., and Riezman, H. (1993). end3 and end4: two mutants defective in receptor-mediated and fluid-phase endocytosis in Saccharomyces cerevisiae. J Cell Biol *120*, 55-65.

65. Shaw, J.D., Cummings, K.B., Huyer, G., Michaelis, S., and Wendland, B. (2001). Yeast as a model system for studying endocytosis. Exp Cell Res *271*, 1-9.

66. Bi, E., Chiavetta, J.B., Chen, H., Chen, G.C., Chan, C.S., and Pringle, J.R. (2000). Identification of novel, evolutionarily conserved Cdc42p-interacting proteins and of redundant pathways linking Cdc24p and Cdc42p to actin polarization in yeast. Mol Biol Cell *11*, 773-793.

67. Howell, A.S., Jin, M., Wu, C.F., Zyla, T.R., Elston, T.C., and Lew, D.J. (2012). Negative feedback enhances robustness in the yeast polarity establishment circuit. Cell *149*, 322-333.

68. Ghaemmaghami, S., Huh, W.K., Bower, K., Howson, R.W., Belle, A., Dephoure, N., O'Shea, E.K., and Weissman, J.S. (2003). Global analysis of protein expression in yeast. Nature *425*, 737-741.

69. Joglekar, A.P., Bouck, D.C., Molk, J.N., Bloom, K.S., and Salmon, E.D. (2006). Molecular architecture of a kinetochore-microtubule attachment site. Nat Cell Biol *8*, 581-585.

70. Joglekar, A.P., Salmon, E.D., and Bloom, K.S. (2008). Counting kinetochore protein numbers in budding yeast using genetically encoded fluorescent proteins. Methods Cell Biol *85*, 127-151.

71. Lawrimore, J., Bloom, K.S., and Salmon, E.D. (2011). Point centromeres contain more than a single centromere-specific Cse4 (CENP-A) nucleosome. J Cell Biol *195*, 573-582.

72. Roumanie, O., Wu, H., Molk, J.N., Rossi, G., Bloom, K., and Brennwald, P. (2005). Rho GTPase regulation of exocytosis in yeast is independent of GTP hydrolysis and polarization of the exocyst complex. J Cell Biol *170*, 583-594.

73. Wu, H., Rossi, G., and Brennwald, P. (2008). The ghost in the machine: small GTPases as spatial regulators of exocytosis. Trends Cell Biol *18*, 397-404.

74. Savage, N.S., Layton, A.T., and Lew, D.J. (2012). Mechanistic mathematical model of polarity in yeast. Mol Biol Cell *23*, 1998-2013.

75. Okada, S., Leda, M., Hanna, J., Savage, N.S., Bi, E., and Goryachev, A.B. (2013). Daughter cell identity emerges from the interplay of Cdc42, septins, and exocytosis. Dev Cell *26*, 148-161.

76. Dyer, J.M., Savage, N.S., Jin, M., Zyla, T.R., Elston, T.C., and Lew, D.J. (2013). Tracking shallow chemical gradients by actin-driven wandering of the polarization site. Curr Biol *23*, 32-41.

77. Slaughter, B.D., Unruh, J.R., Das, A., Smith, S.E., Rubinstein, B., and Li, R. (2013). Non-uniform membrane diffusion enables steady-state cell polarization via vesicular trafficking. Nat Commun *4*, 1380.

78. Hoffman, C.S. (2001). Preparation of yeast DNA. Curr Protoc Mol Biol *Chapter 13*, Unit13 11.

79. Moerschell, R.P., Das, G., Sherman, F., and Christine Guthrie, G.R.F. (1991). [24] Transformation of yeast directly with synthetic oligonucleotides. In Methods in Enzymology, Volume Volume 194. (Academic Press), pp. 362-369.

80. Brennwald, P., and Novick, P. (1993). Interactions of three domains distinguishing the Ras-related GTP-binding proteins Ypt1 and Sec4. Nature *362*, 560-563.

81. Schneider, C.A., Rasband, W.S., and Eliceiri, K.W. NIH Image to ImageJ: 25 years of image analysis. Nat Methods *9*, 671-675.

82. Sprague, B.L., Pearson, C.G., Maddox, P.S., Bloom, K.S., Salmon, E.D., and Odde, D.J. (2003). Mechanisms of microtubule-based kinetochore positioning in the yeast metaphase spindle. Biophys J *84*, 3529-3546.

83. Adams, A.E., and Pringle, J.R. (1984). Relationship of actin and tubulin distribution to bud growth in wild-type and morphogenetic-mutant Saccharomyces cerevisiae. J Cell Biol *98*, 934-945.

84. Kilmartin, J.V., and Adams, A.E. (1984). Structural rearrangements of tubulin and actin during the cell cycle of the yeast Saccharomyces. J Cell Biol *98*, 922-933.

85. Lewis, M.J., Nichols, B.J., Prescianotto-Baschong, C., Riezman, H., and Pelham, H.R. (2000). Specific retrieval of the exocytic SNARE Snc1p from early yeast endosomes. Mol Biol Cell *11*, 23-38.

86. Bryant, N.J., and Stevens, T.H. (1997). Two separate signals act independently to localize a yeast late Golgi membrane protein through a combination of retrieval and retention. J Cell Biol *136*, 287-297.

87. Holthuis, J.C., Nichols, B.J., and Pelham, H.R. (1998). The syntaxin Tlg1p mediates trafficking of chitin synthase III to polarized growth sites in yeast. Mol Biol Cell *9*, 3383-3397.

88. Ziman, M., Chuang, J.S., and Schekman, R.W. (1996). Chs1p and Chs3p, two proteins involved in chitin synthesis, populate a compartment of the Saccharomyces cerevisiae endocytic pathway. Mol Biol Cell *7*, 1909-1919.

89. Ziman, M., Chuang, J.S., Tsung, M., Hamamoto, S., and Schekman, R. (1998). Chs6p-dependent anterograde transport of Chs3p from the chitosome to the plasma membrane in Saccharomyces cerevisiae. Mol Biol Cell *9*, 1565-1576.

90. Hicke, L., and Riezman, H. (1996). Ubiquitination of a yeast plasma membrane receptor signals its ligand-stimulated endocytosis. Cell *84*, 277-287.

91. Rohrer, J., Benedetti, H., Zanolari, B., and Riezman, H. (1993). Identification of a novel sequence mediating regulated endocytosis of the G protein-coupled alpha-pheromone receptor in yeast. Mol Biol Cell *4*, 511-521.

92. Adamo, J.E., Moskow, J.J., Gladfelter, A.S., Viterbo, D., Lew, D.J., and Brennwald, P.J. (2001). Yeast Cdc42 functions at a late step in exocytosis, specifically during polarized growth of the emerging bud. J Cell Biol *155*, 581-592.

93. Caviston, J.P., Longtine, M., Pringle, J.R., and Bi, E. (2003). The role of Cdc42p GTPase-activating proteins in assembly of the septin ring in yeast. Mol Biol Cell *14*, 4051-4066.

94. Gladfelter, A.S., Bose, I., Zyla, T.R., Bardes, E.S., and Lew, D.J. (2002). Septin ring assembly involves cycles of GTP loading and hydrolysis by Cdc42p. J Cell Biol *156*, 315-326.